Compiled pictures from Simpson's Forensic Medicine 13th edition

Note:
The following pictures were not found on the PDF book.
pg 63
pg 69
pg 71
pg 73
pg 105
pg 144
pg 152

Chapter 3: The medical aspects of death

Figure 3.2 Examination of skeletal remains at a wooded 'scene'. The forensic pathologist wears appropriate protective equipment in order to prevent contamination of the remains. The attendance at a 'scene' follows discussion with the crime scene manager regarding the health and safety implications of the 'scene', the approach to the body/remains and a forensic strategy for the recovery of 'trace evidence', including swabs and 'tape lifts' from sites such as exposed skin surfaces and body orifices.

Figure 3.3 Modern forensic autopsy facilities, including directional overhead lighting – with inbuilt video projection and recording capability – to facilitate optimal forensic pathological examinations.

Figure 3.4 Operating microscopy in the forensic autopsy suite facilitates detailed examination and documentation of pathological findings.

Figure 3.5 Post-mortem radiology is important in many cases in forensic pathology. Note the body is enclosed in a body bag to prevent contamination of the body and loss of 'trace evidence' from the surface of the body, prior to autopsy. Hands (and usually feet) are similarly protected by paper or plastic bags before recovery of a body from a scene.

Figure 3.6 Removal of the coffin lid following an exhumation. Liquid mud covers the upper body following leakage of the coffin lid.

Chapter 4: Identification of the living and the dead

Figure 4.2 Retained dentition after fire.

Chapter 5: The appearance of the body after death

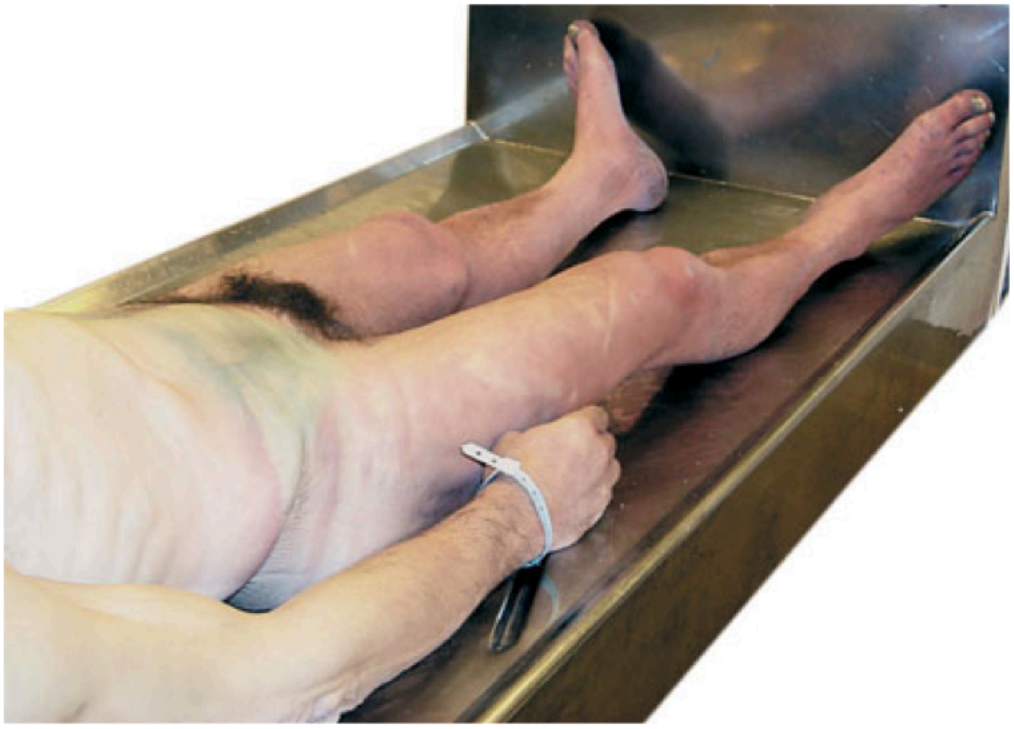

Figure 5.3 Post-mortem hypostasis distribution following hanging. Note the skin discoloration is in the legs and hands because of the vertical body position after death and the green discoloration in the right iliac fossa region.

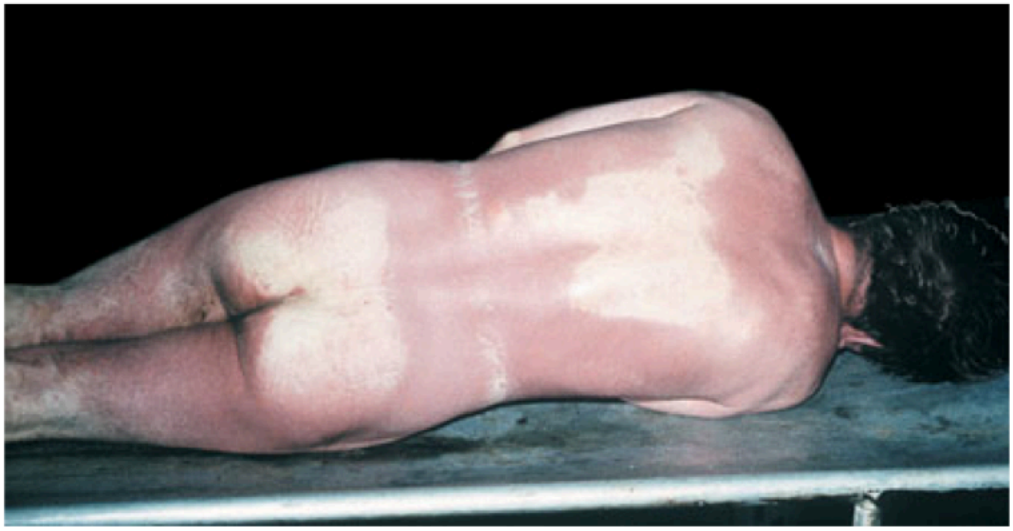

Figure 5.2 Post-mortem hypostasis in a posterior distribution. Areas of pallor can be seen as a result of pressure of the body on a firm surface, whereas parts of the body not in direct contact with that surface are purple/ pink because of the 'settling of blood under gravity'. This body has been lying on its back since death.

Figure 5.4 Post-mortem hypostasis pattern on the front of a body found face down on a bed. The linear marks are formed by pressure from creases in a blanket. Pallor around the mouth and nose are caused by pressure against the bed and do not necessarily indicate marks of suffocation.

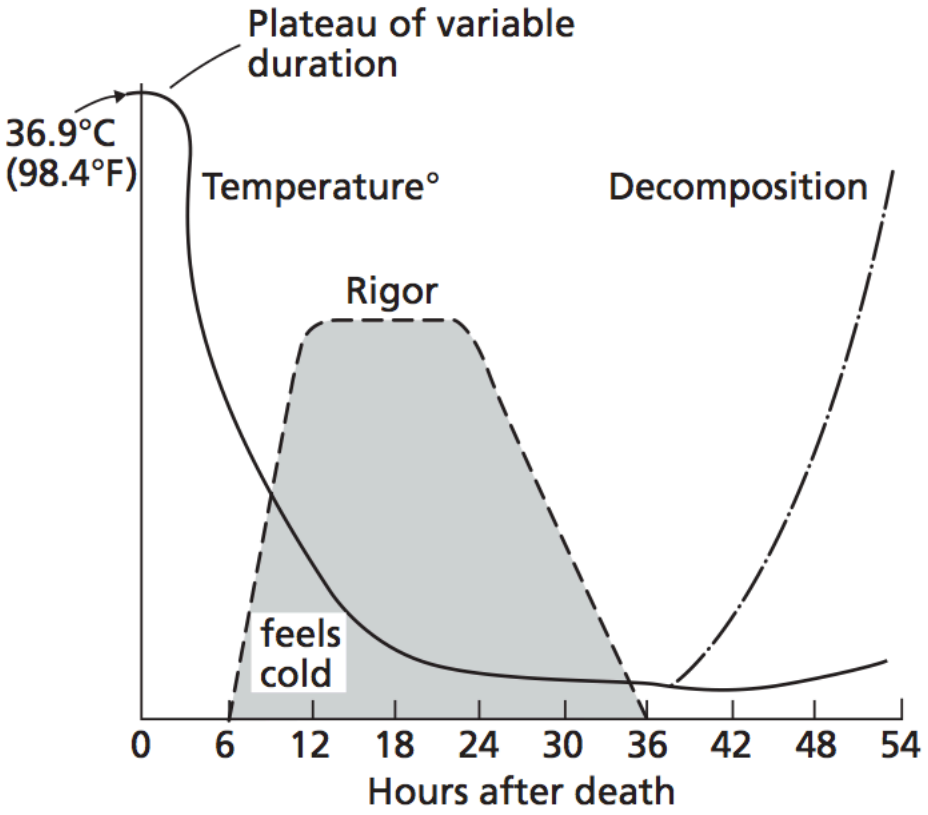

Figure 5.5 The sequence of major changes after death in a temperate environment. Note that the core body temperature does not show a fall for the first hour or so.

Figure 5.6 Early decomposition with skin slippage and discoloration. Note the 'marbling' representing discoloration owing to decomposition within superficial blood vessels.

Figure 5.7 Putrefaction/decomposition of approximately 1 week in temperate summer conditions. Note the 'bloating' of soft tissues, distortion of facial features and 'purge fluid' emanating from the mouth and nose.

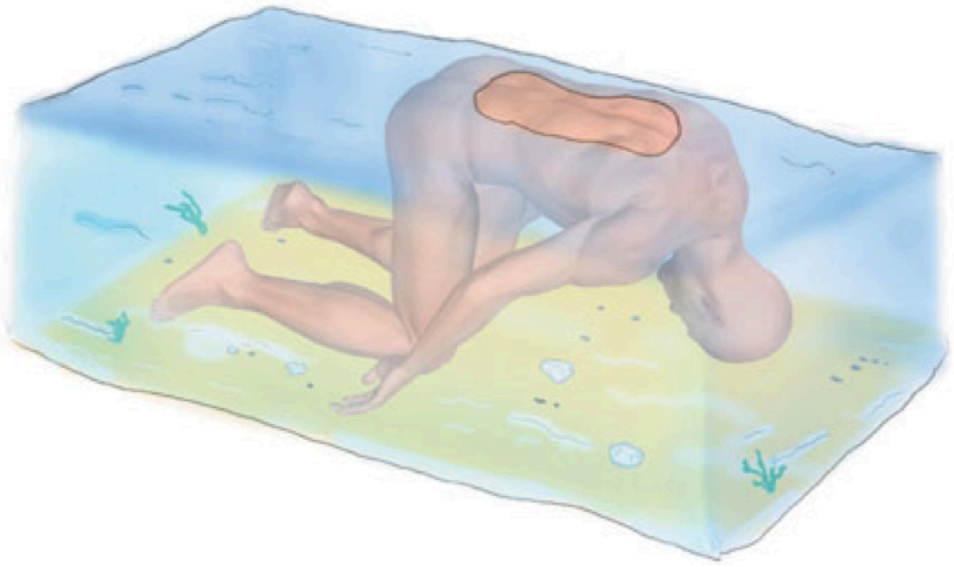

Figure 5.8 Disposition of a body floating in water. Typically the head and limbs hang down, resulting in superficial injuries to the head/ face, back of the arms and hands, knees and top of the feet.

Figure 5.9 Marine creature predation in a body recovered from the North Sea after 3 months. Much of the skin has been removed by crustaceans, and the arm muscles by larger fish who have cleaned out most of the body cavity.

Figure 5.10 Adipocere formation. Following burial for 3 years, waxy adipocere forms a shell around the skeleton of this infant.

Figure 5.11 Mummification. The skin is dry and leathery following recovery from a locked room for 10 weeks.

Figure 5.12 Post-mortem animal predation. The wound margins of these rat bites are free from haemorrhage or reddening. Such injuries are commonly present around the eyes, ears and nose.

Figure 5.13 Maggot infestation of a body recovered from heated premises approximately 2 weeks after death. Forensic entomology may assist in estimating post-mortem interval (PMI) in such cases.

Chapter 6: Unexpected and sudden death from natural causes

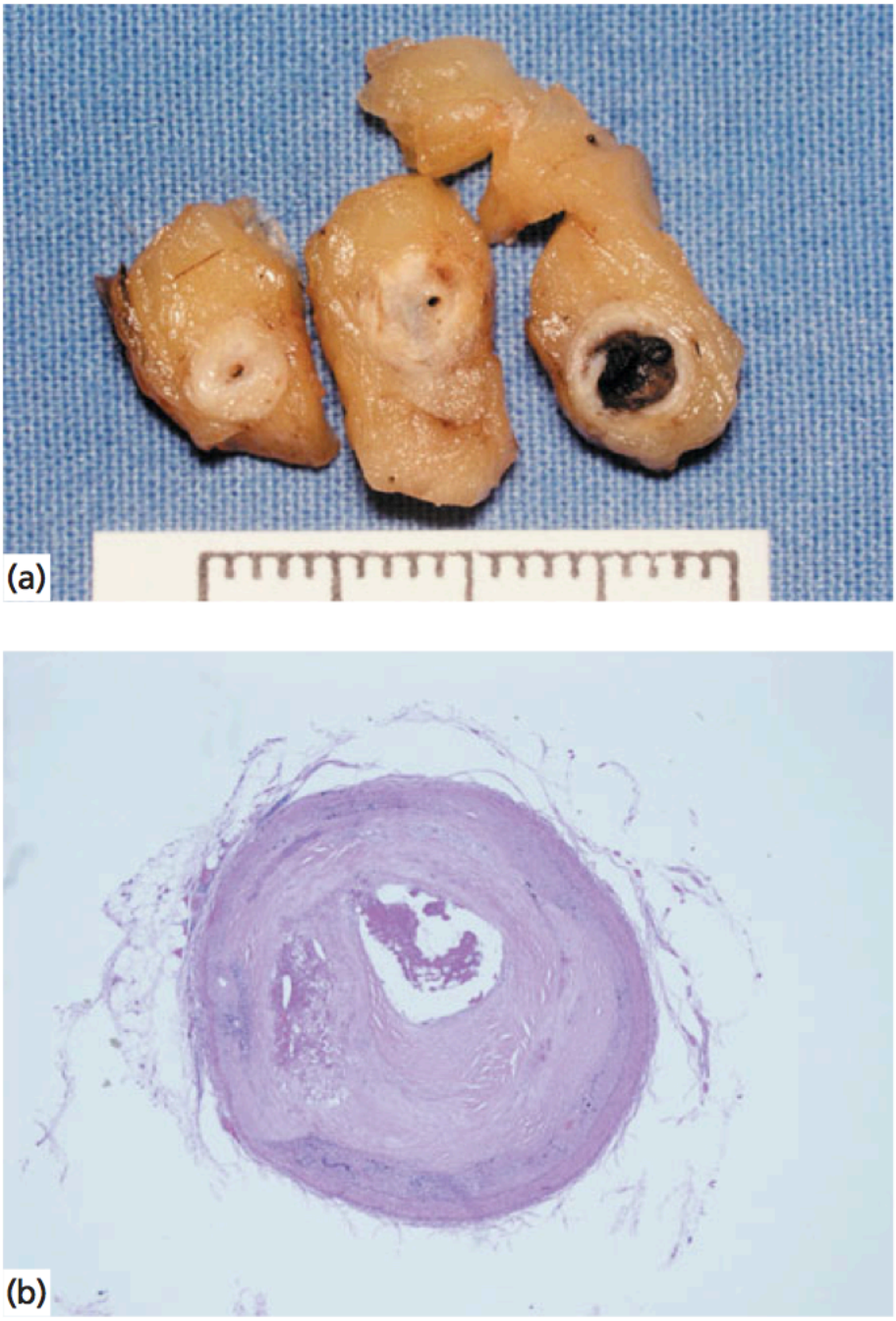

Figure 6.1 Significant coronary artery atherosclerosis and acute thrombosis. Macroscopic **(a)** and microscopic **(b)** appearance.

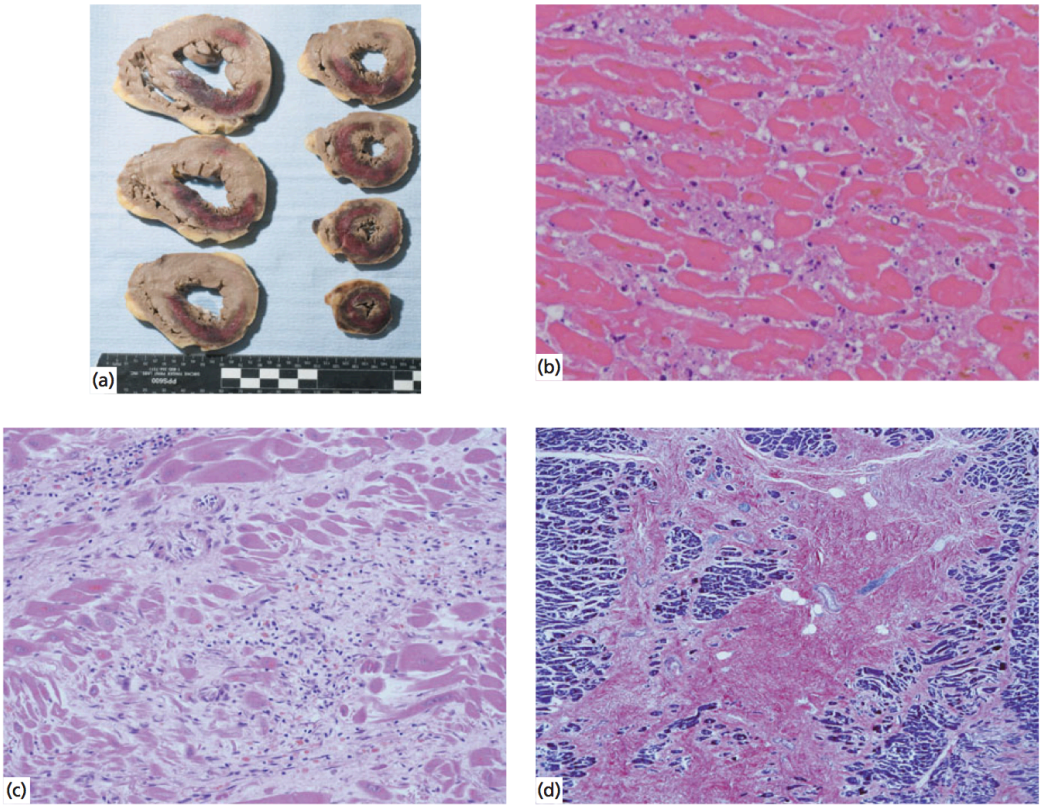

Figure 6.2 Myocardial infarction. **(a)** Macroscopic appearance of acute left-ventricular myocardial infarction. **(b–d)** Microscopic appearance of myocardial infarction with early necrosis **(b)**, organization including residual haemosiderin-laden macrophages and fibroblasts **(c)**, and extensive replacement fibrosis **(d)**.

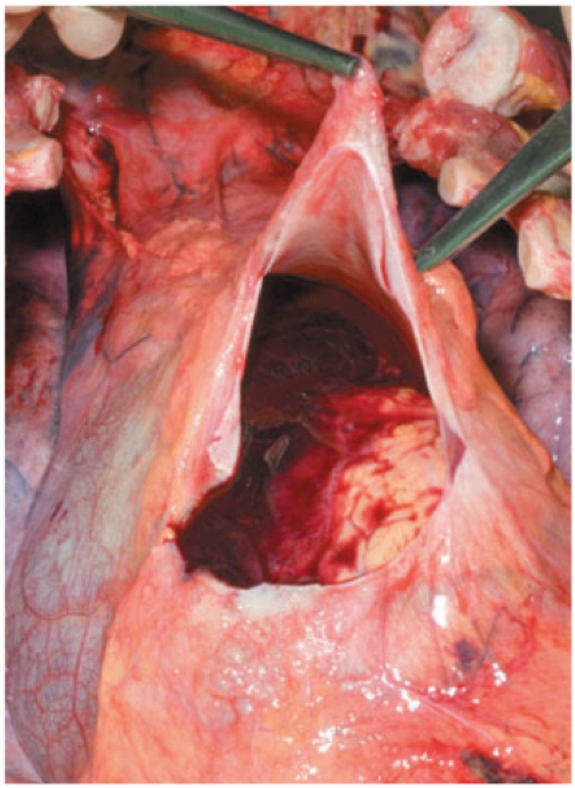

Figure 6.3 Haemopericardium causing cardiac tamponade. The distended pericardial sac has been opened to reveal fluid and clotted blood.

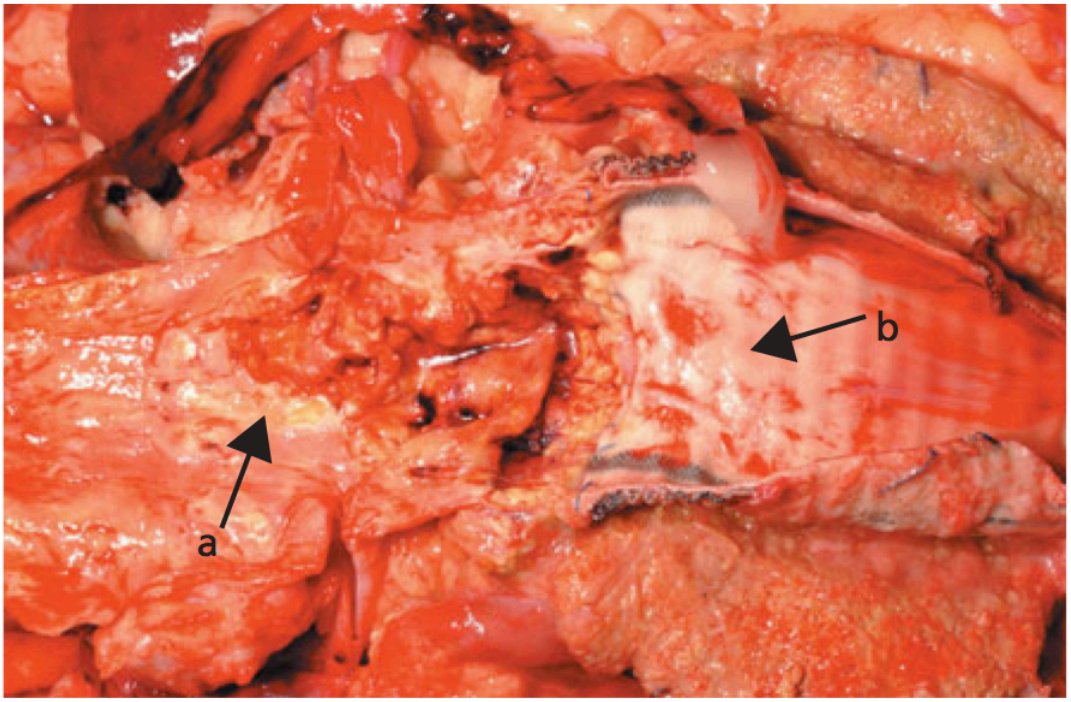

Figure 6.4 Atherosclerotic abdominal aortic aneurysm. As the aneurysm dilates, there is an increased risk of leakage and frank rupture, leading to fatal intra-abdominal or retroperitoneal haemorrhage. **a** Ulcerated atherosclerotic plaque; **b** Site of previous aneurysm repair.

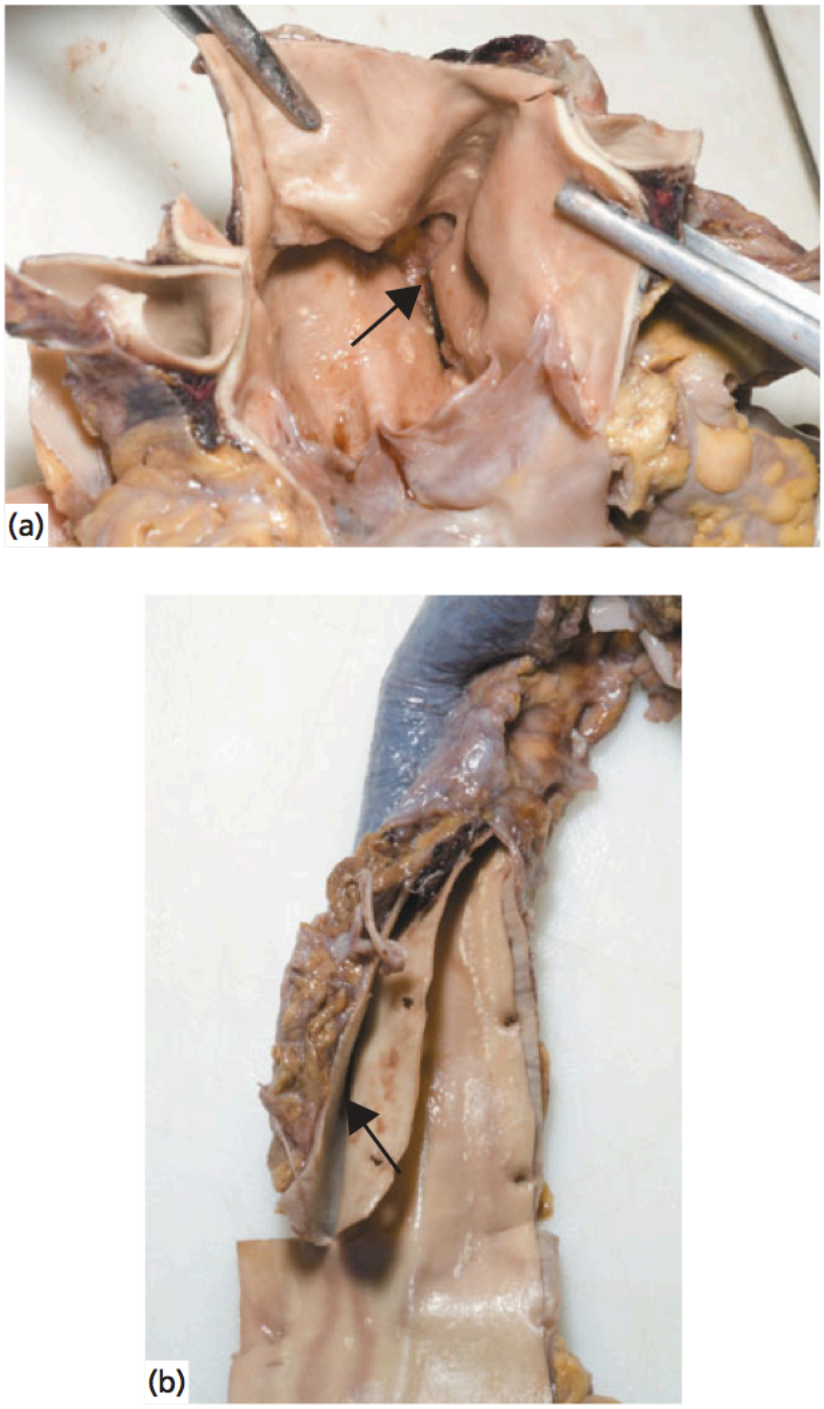

Figure 6.5 Thoracic aortic dissection. The origin of the dissection is in the aortic root, just above the tricuspid aortic valve **(a)** with a plane of dissection in the aortic media **(b)**.

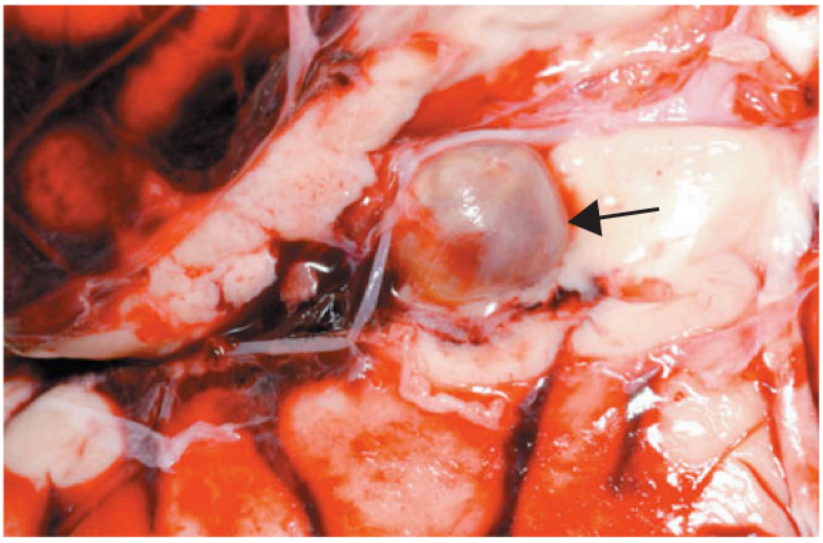

Figure 6.6 Berry aneurysm of the proximal middle cerebral artery and associated subarachnoid haemorrhage.

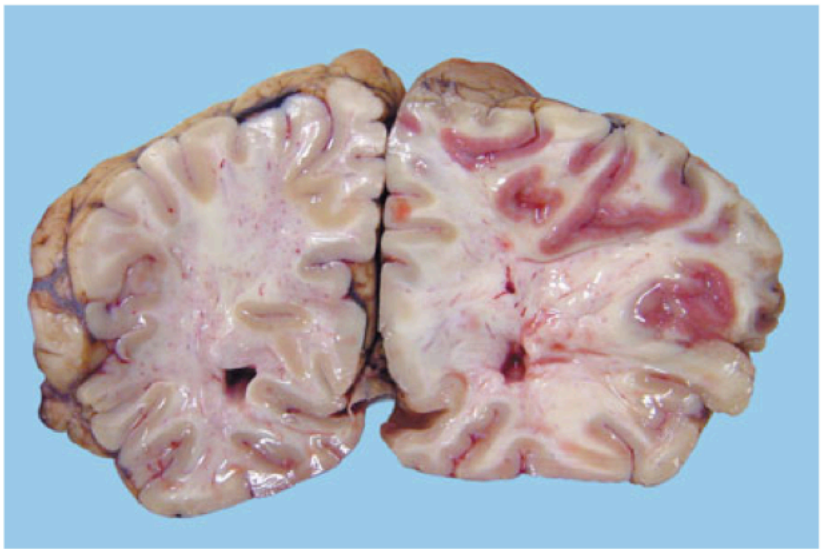

Figure 6.7 Acute cerebral infarction (predominantly middle cerebral artery territory).

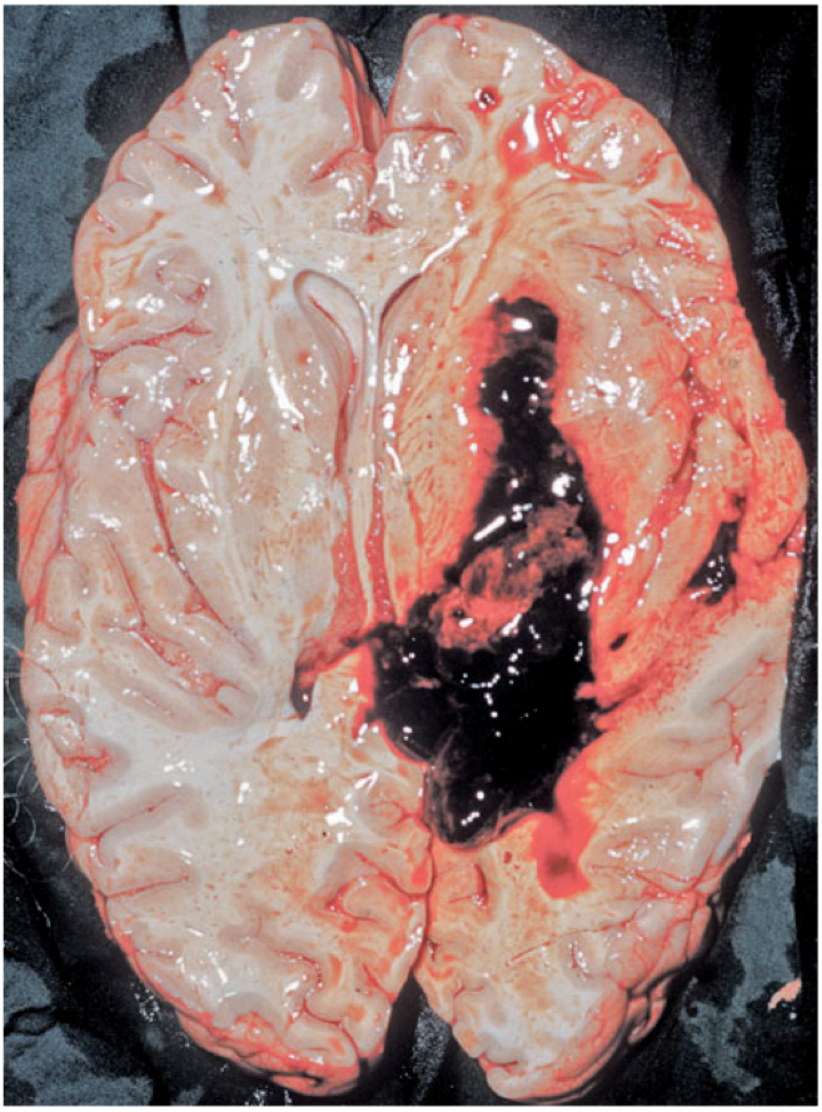

Figure 6.8 Recent intracerebral haemorrhage in a hypertensive individual.

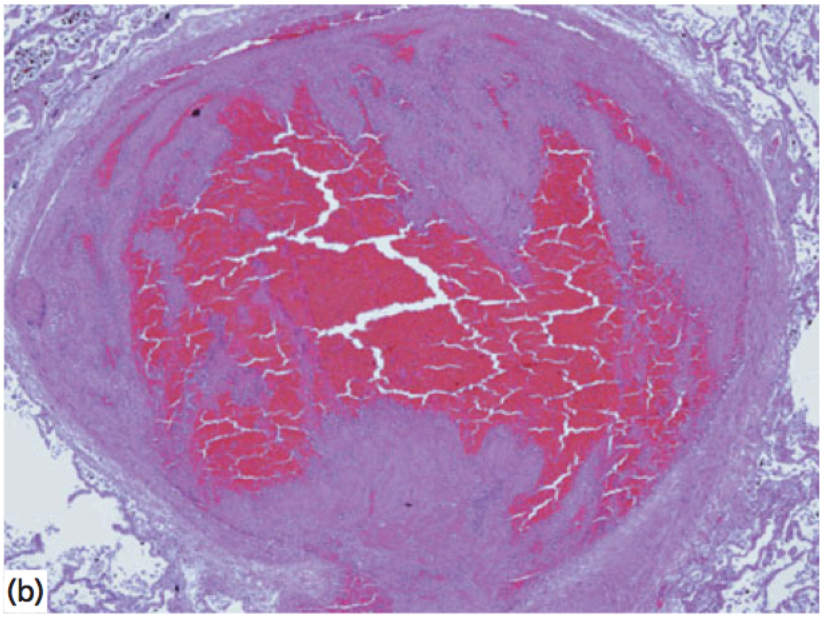

Figure 6.9 Fatal pulmonary thromboembolism. Macroscopic **(a)** and microscopic **(b)** appearance.

Figure 6.10 Disseminated pulmonary tuberculosis (TB). Note also the cavitating (secondary TB) lesion.

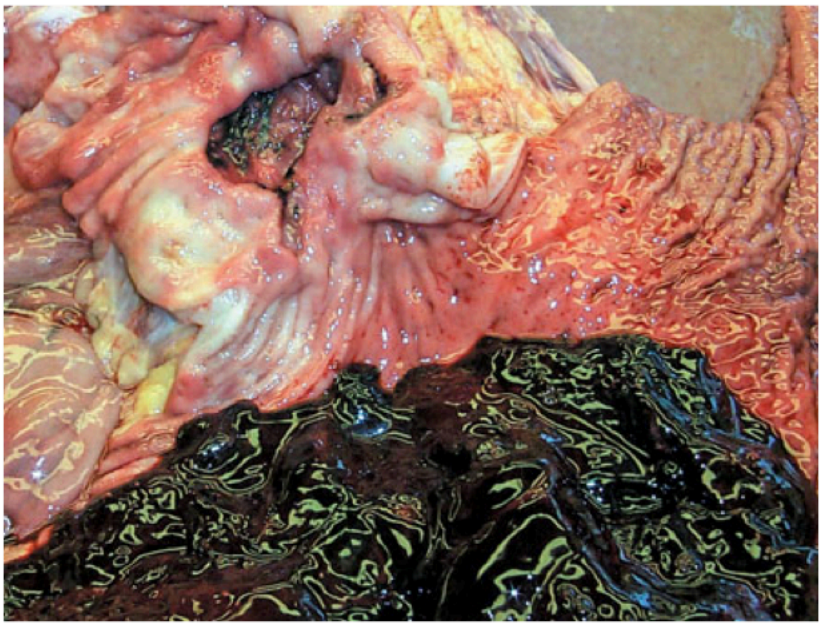

Figure 6.11 Massive haemorrhage from erosion of blood vessels in the base of this peptic gastric ulcer.

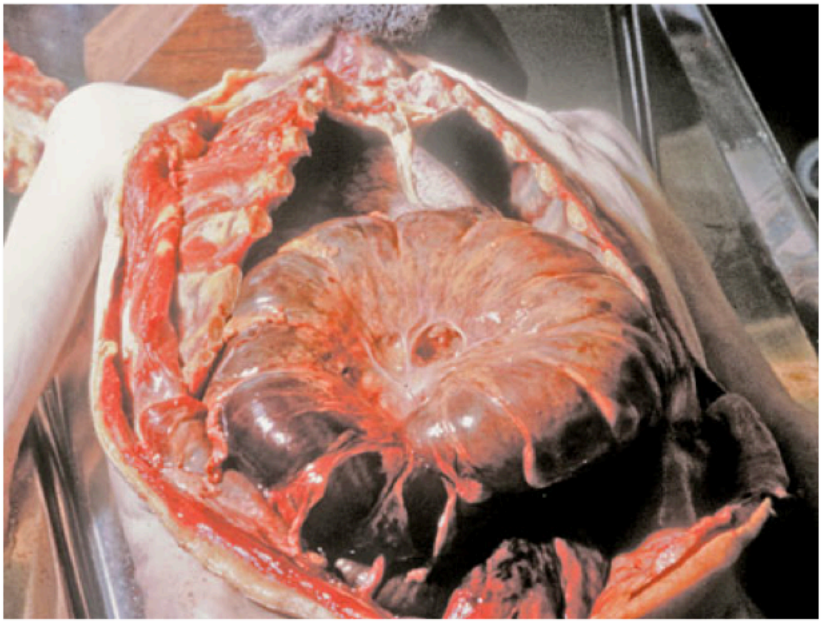

Figure 6.12 Intestinal infarction following volvulus of the sigmoid colon.

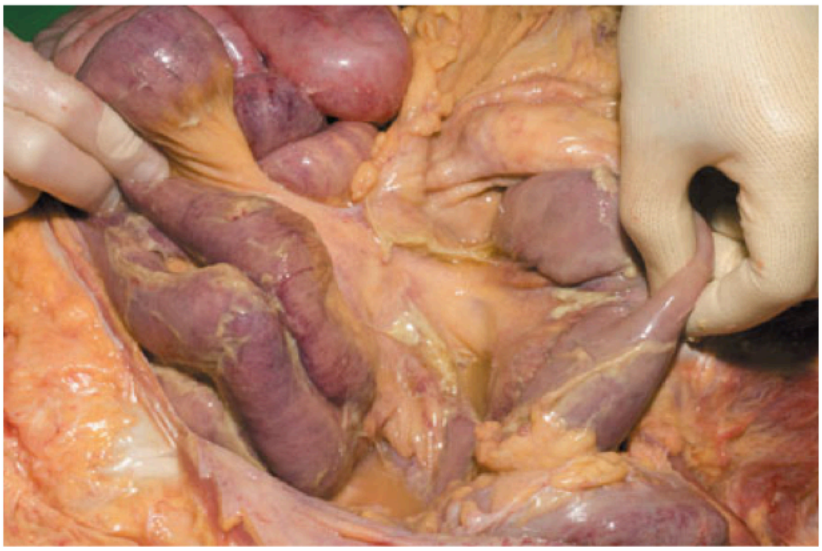

Figure 6.13 Peritonitis. Note the fibrinous deposits on the surface of loops of intestines.

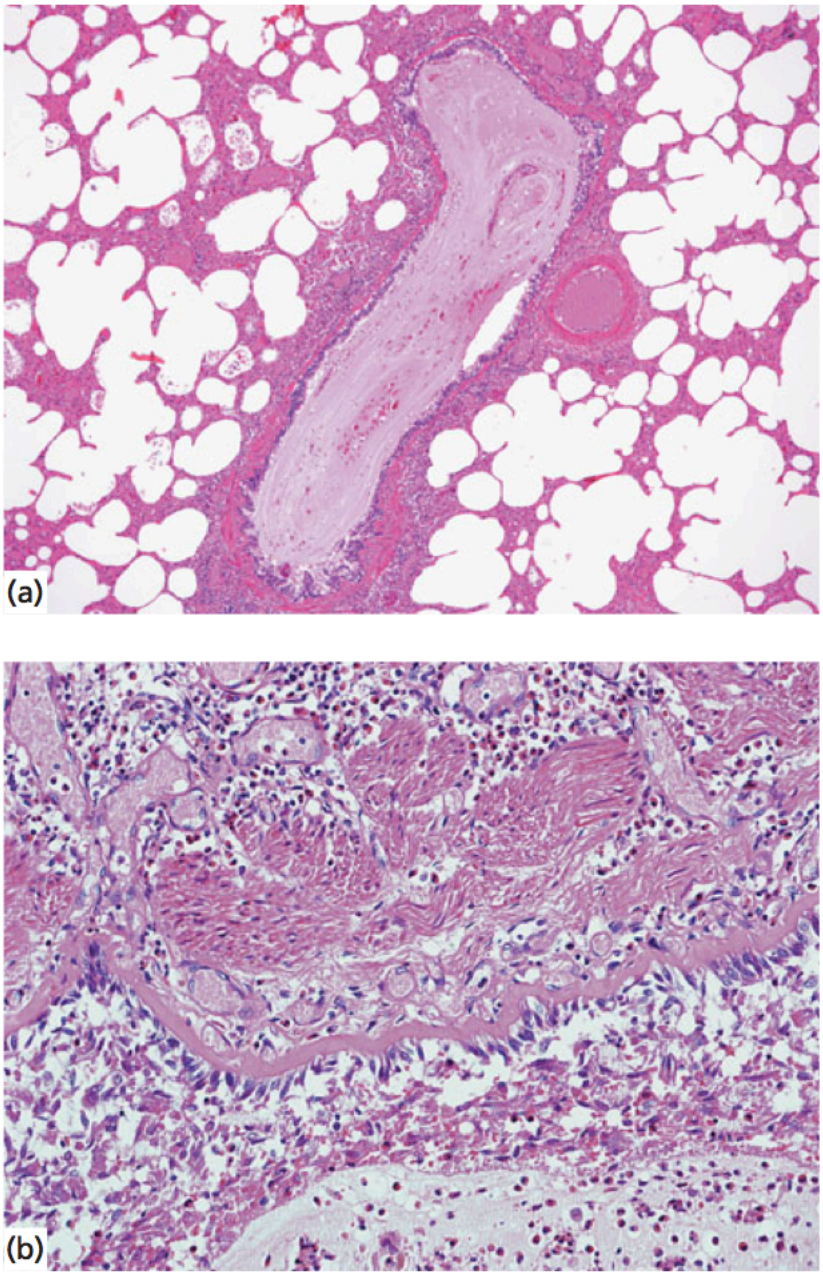

Figure 6.15 Bronchial asthma. **(a,b)** Microscopy demonstrating airway 'remodelling', mucus distension and inflammatory cell infiltration, including neutrophils and eosinophils.

Chapter 7: Death and injury in infancy

Figure 7.1 Maceration following intrauterine death. Note the widespread skin slippage and the umbilical cord around the neck.

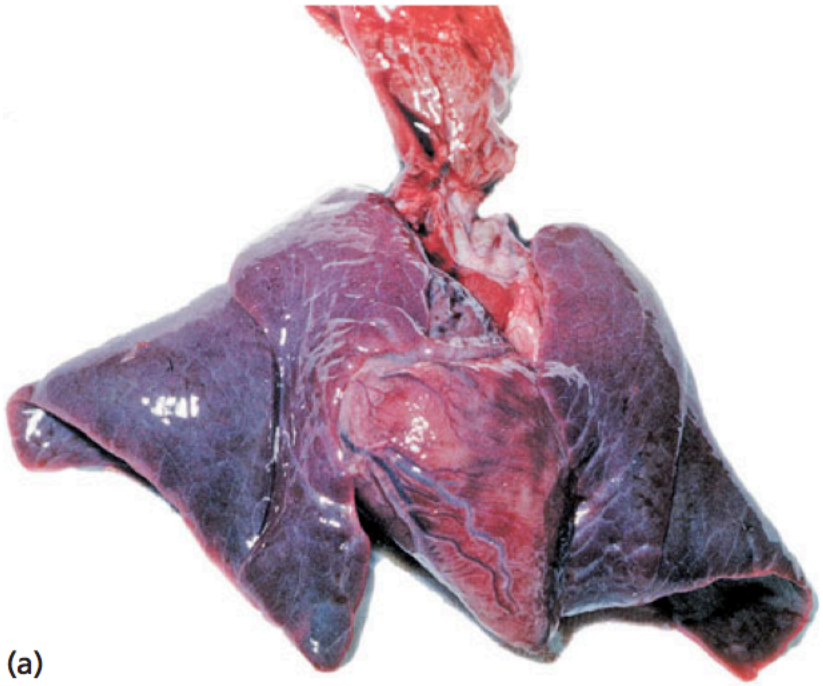

(a)

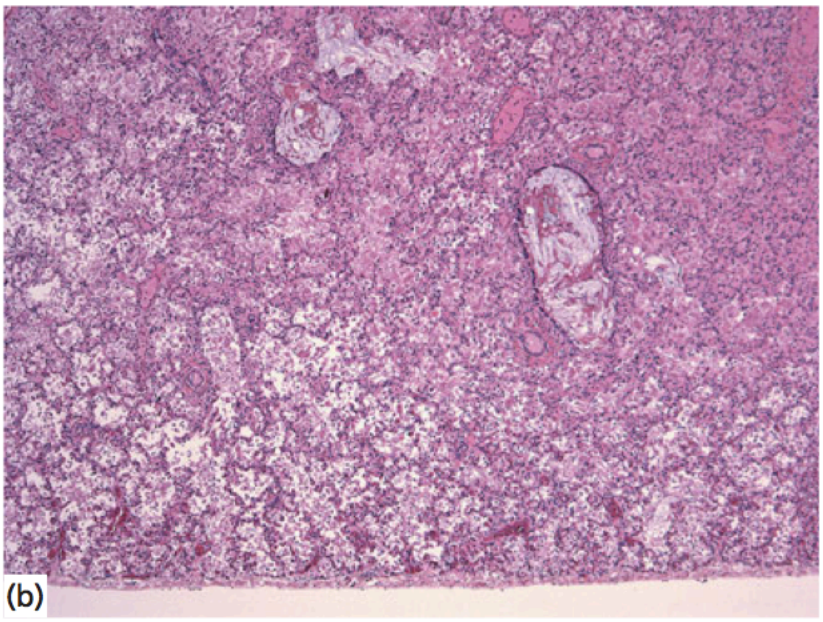

(b)

Figure 7.2 **(a)** Thoracic organs from a stillbirth. The lungs are firm and heavy with no crepitation when squeezed. **(b)** Microscopy of lungs from stillbirths showing partial expansion of terminal air spaces as a consequence of hypoxia-induced inspiratory efforts. Note also meconium aspiration.

Figure 7.3 Newborn infant disposal with decompositional/ putrefactive skin changes.

Figure 7.5 Multiple 'fingertip' bruises on the front of the trunk in an abused infant.

Figure 7.6 Ear bruising in an infant raises the possibility of non-accidental injury. Radiology revealed multiple rib fractures.

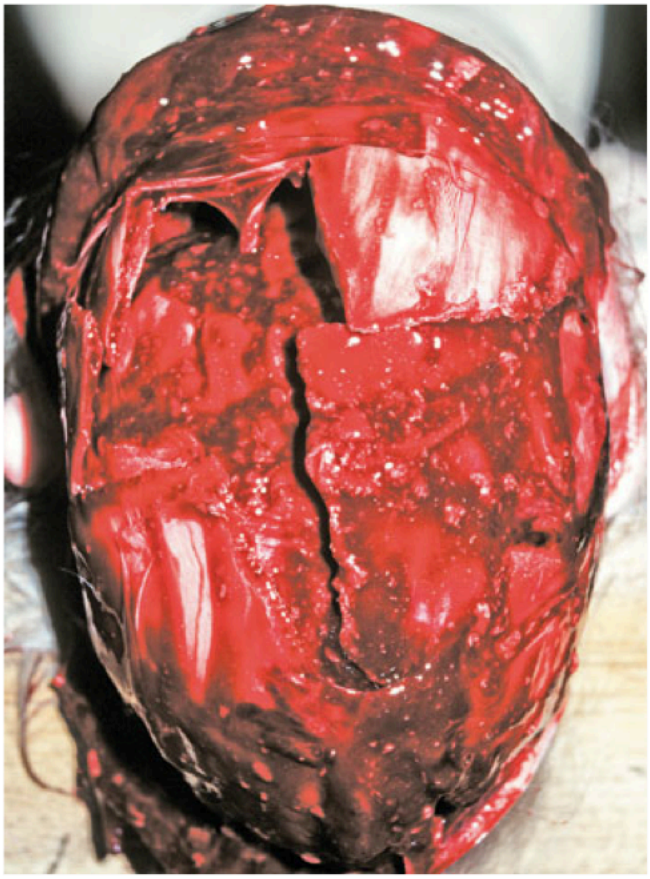

Figure 7.8 Multiple skull fractures following blunt force impacts against the floor.

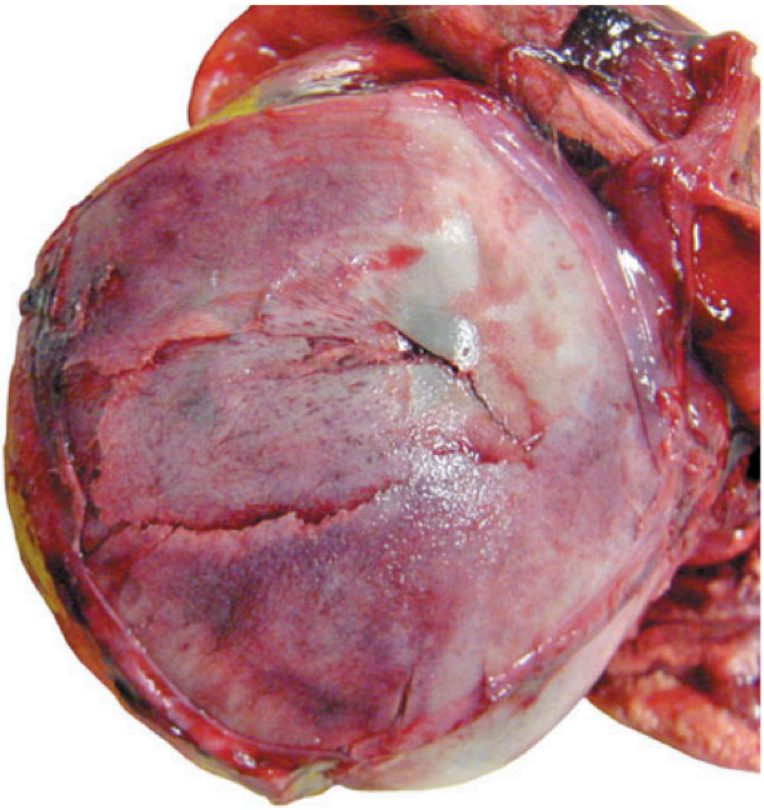

Figure 7.9 Depressed skull fracture. Not all infant skull fractures are non-accidental in origin; instrumentation and manual dis-impaction from the birth canal led to this fracture.

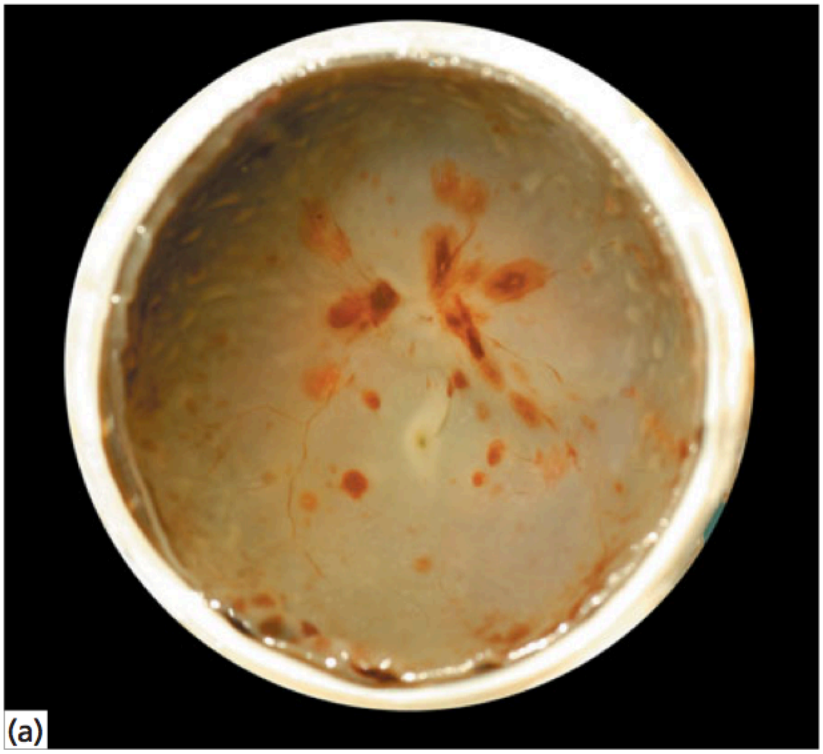

Figure 7.10 Retinal haemorrhages **(a)** macroscopic post-mortem a
haemorrhage within multiple layers of the retina. (i) Vitreous body; (i

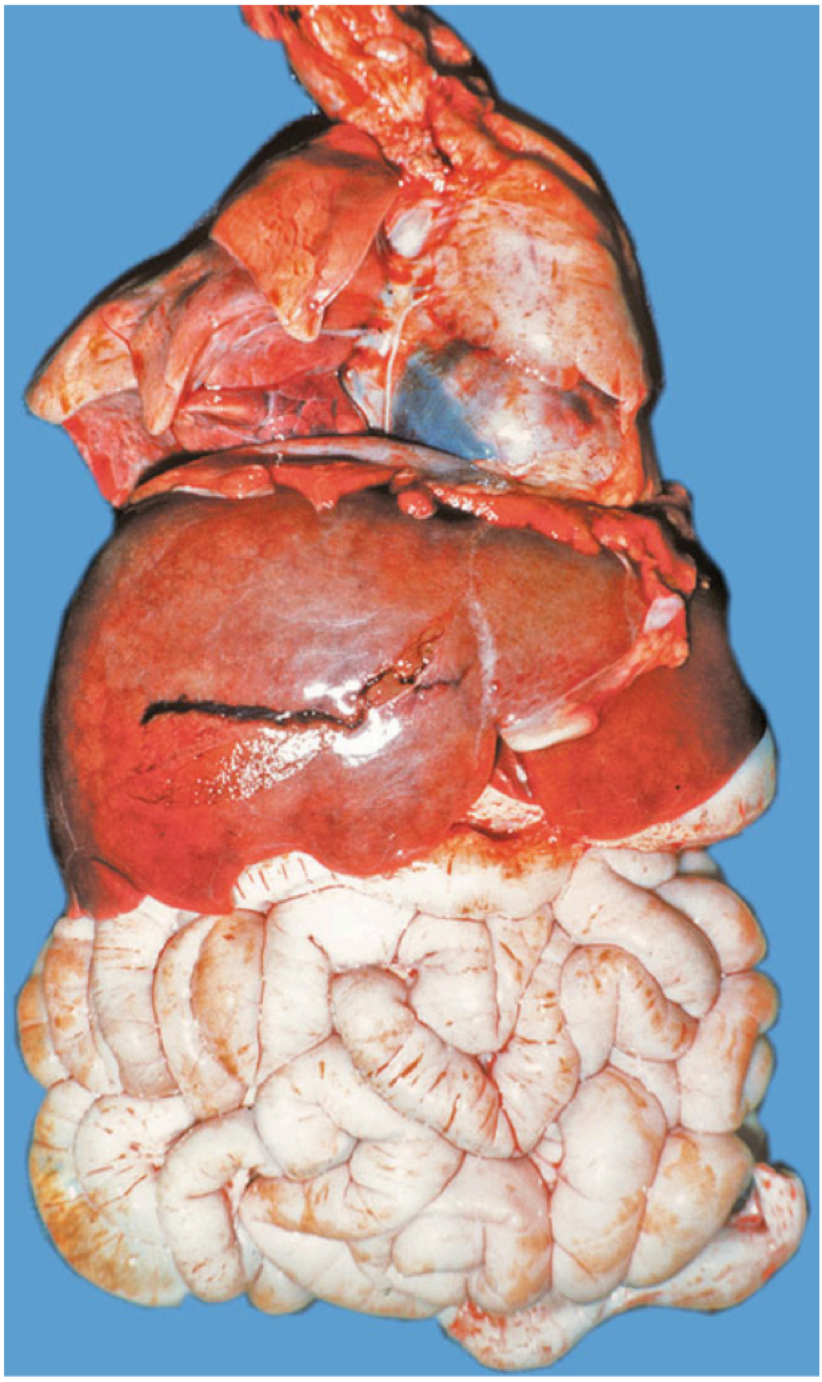

Figure 7.12 Non-accidental, blunt force, intra-abdominal visceral injury (same infant as in Figure 7.5). Note the liver laceration leading to intra-abdominal haemorrhage.

Chapter 8: Assessment, classification and documentation of injury

Figure 8.1 Reddening (erythema) related to blunt impact at outer aspect of left eye.

Figure 8.2 Marked swelling (oedema) following multiple punches to left side of face.

Figure 8.3 Bruising (contusion) to thigh **(a)** following direct blunt force impact (fall between iron girders). **(b)** Shows resolution of bruising 5 days after injury as seen in 8.3(a). **(c)** Bruising to leg from multiple blunt impacts with a piece of wood.

Figure 8.4 **(a)** Variable depth abrasions (grazes) caused by impact against concrete surface. **(b)** Linear abrasions caused by fingernail scratching on torso.

Figure 8.5 Laceration, with irregular edges, maceration and skin bridging caused by direct impact to forehead with wooden pole.

Figure 8.7 **(a)** Close-up of face after manual strangulation 2 hours after compression with multiple petechial bruising over facial skin. **(b)** Scleral blood, caused by coalescence of multiple petechiae, 36 hours after manual strangulation.

Figure 8.8 Classical love or 'hickey' bite – bruising to neck caused by suction.

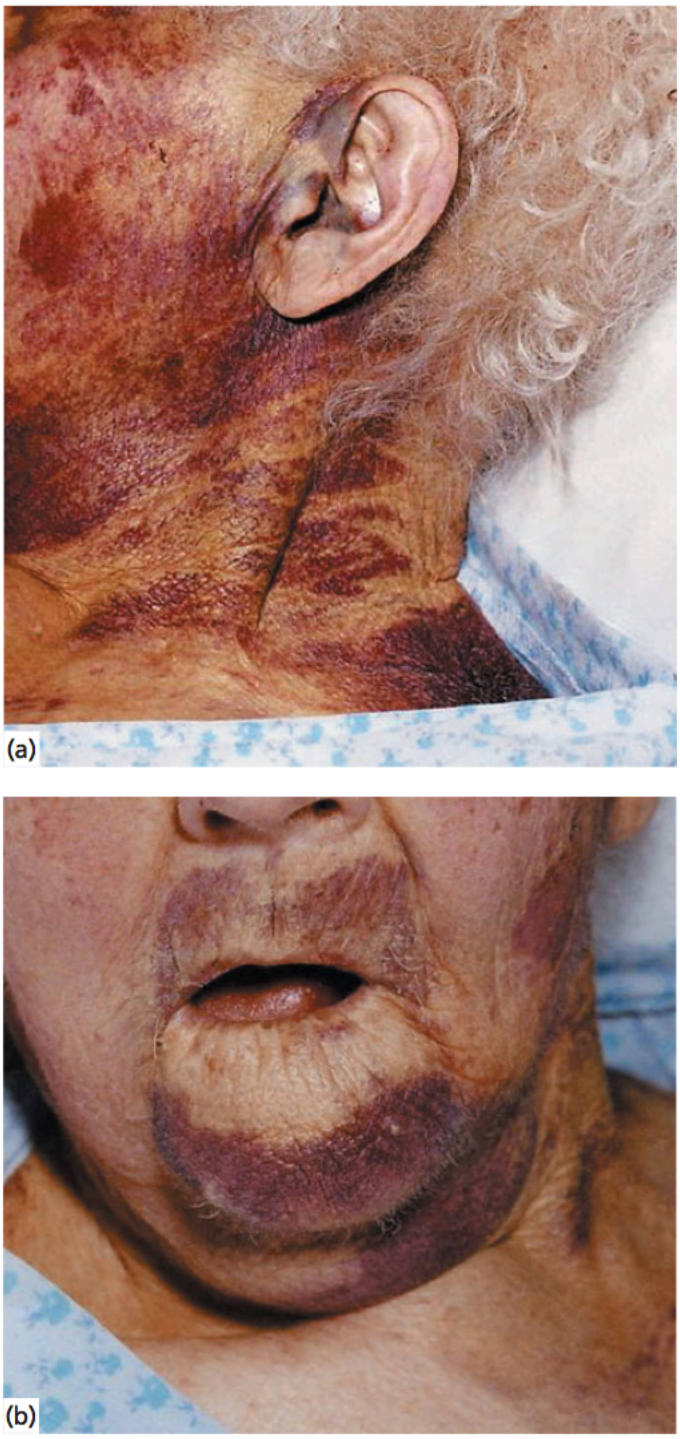

Figure 8.9 Extensive bruising following tissue planes and contours, one week after multiple blunt force impacts to **(a)** head and **(b)** face (neck was spared impacts).

Figure 8.10 **(a)** Patterned bruise – intradermal bruising caused by stamping on back with textured clothing intervening. **(b)** Patterned bruise caused by impact of dog chain. **(c)** Patterned bruise (bruise obliquely towards midline) caused by impact of 2 × 2 length of wood.

Figure 8.11 Tramline bruise caused by impact from cylindrical firm object (in this case, a police baton).

Figure 8.12 Shoeprint bruise following stamping injury to face.

Figure 8.13 Grip marks from fingers on assailant bruises from grip and abrasions from fingernails seen on upper inner arm.

Figure 8.15 Ligature mark with parchmented abrasion in posterior part of neck.

Figure 8.14 Abrasion to right face and cheek caused by kick from shod foot. Linearity of abrasion assists in determining direction of movement.

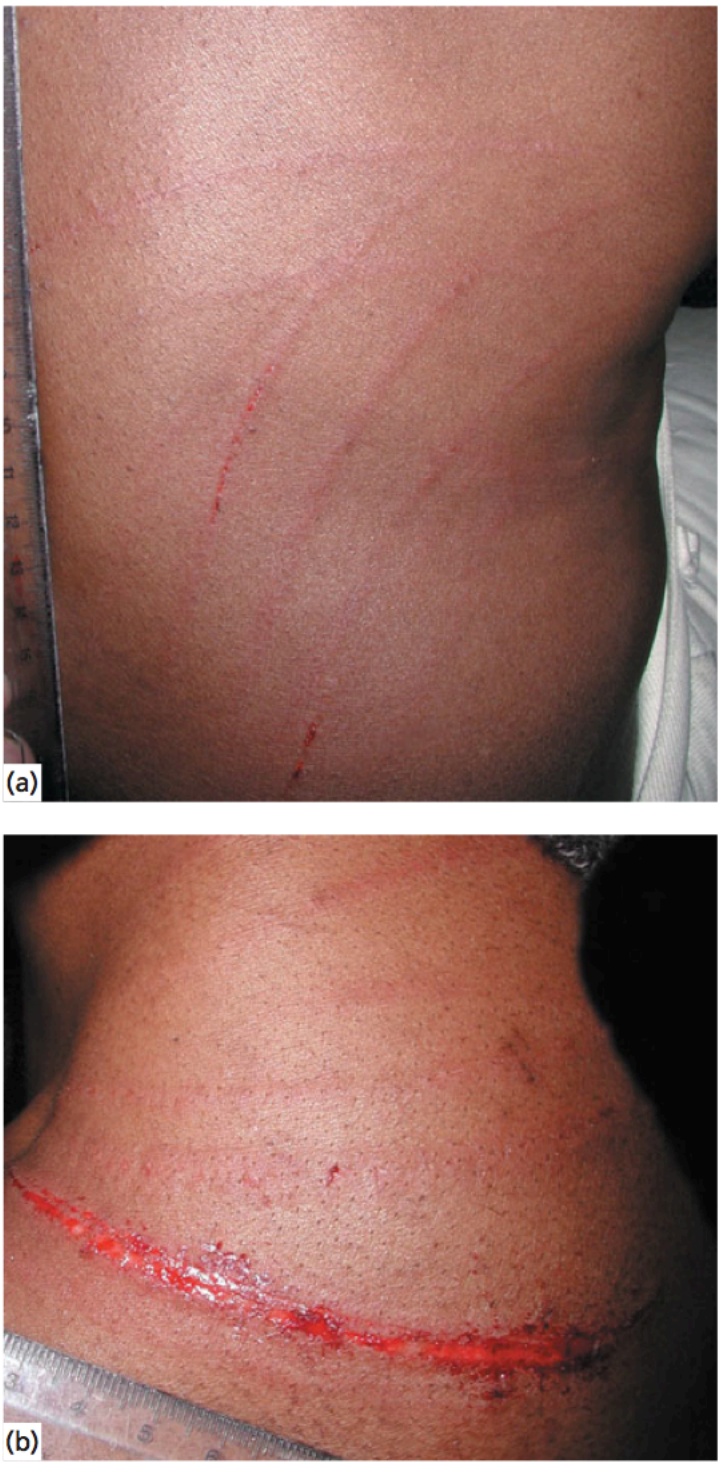

Figure 8.16a **(a)** Multiple fingernail scratches with wheal reaction and superficial abrasions. **(b)** Deeper abrasions caused by fingernails.

Figure 8.17 Close-up showing tags of elevated skin in scuff abrasions.

Figure 8.18 Deep linear point or gouge abrasions to forehead.

Figure 8.19 Deep and extensive abrasion ('gravel rash') caused by contact with road surface after motorcycle accident.

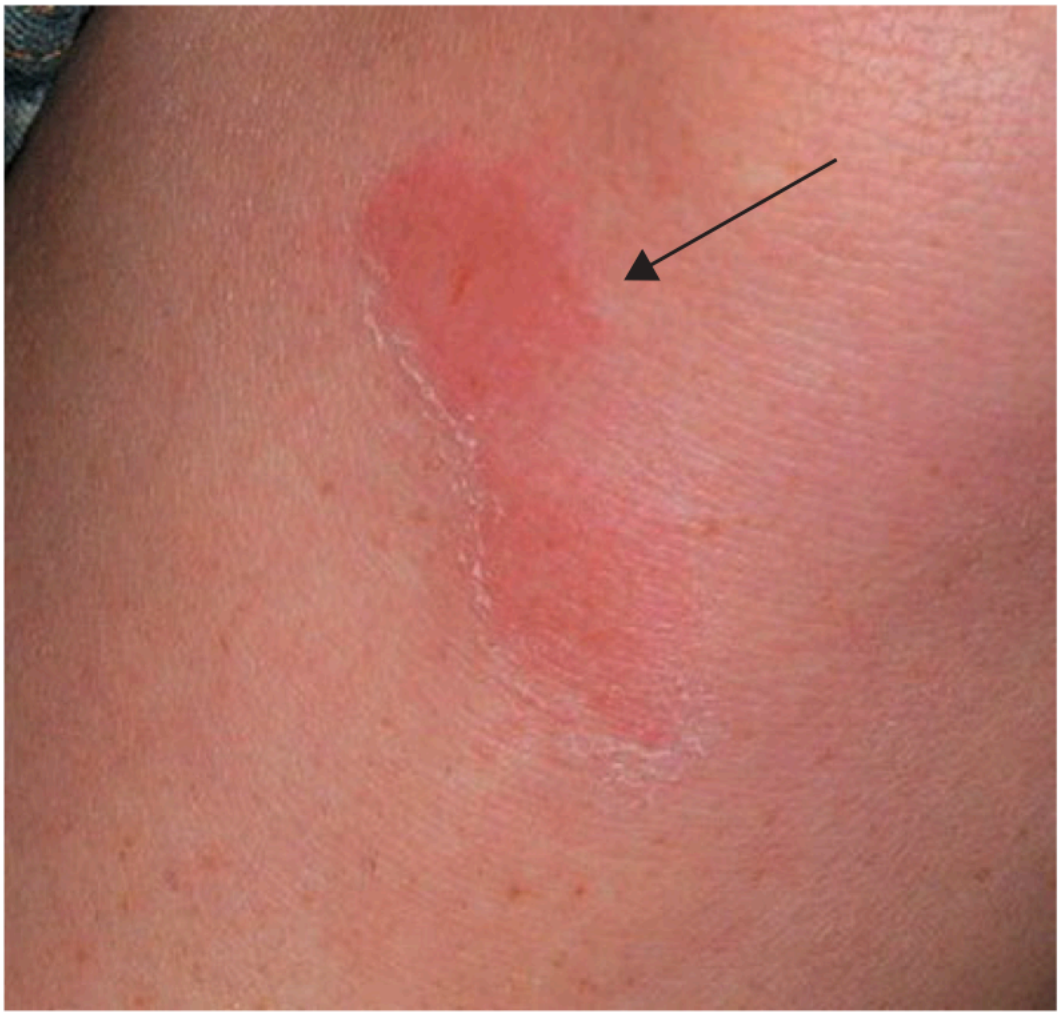

Figure 8.20 Directional scuff – note raised skin layers on left side of abrasion: arrow indicates direction of abrasive movement.

Figure 8.21 Laceration to ear following impact with baseball bat – note irregularity of laceration and associated swelling bruising masked by dry blood.

Figure 8.22 **(a)** Sutured incised wound caused by razor blade – note how wound follows contours. **(b)** Incised wound caused by knife drawn across surface of fingers in this case contours are spared.

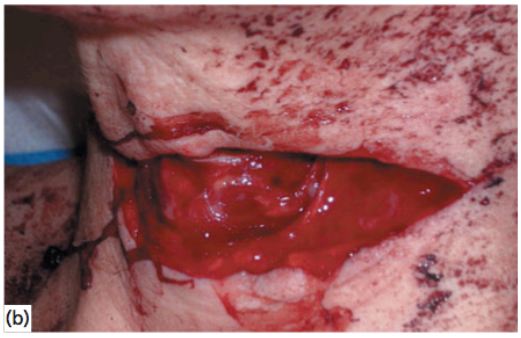

Figure 8.23 **(a)** Sutured incised wound across right side of head and face. **(b)** Incised wound to neck caused by use of knife. **(c)** Irregular incised wounds caused by glass impacted and breaking on face. **(d)** Post-treatment appearance after glassing – note multiple small superficial shard cuts in association with larger incised wounds.

of factors determine how much force is required, including:

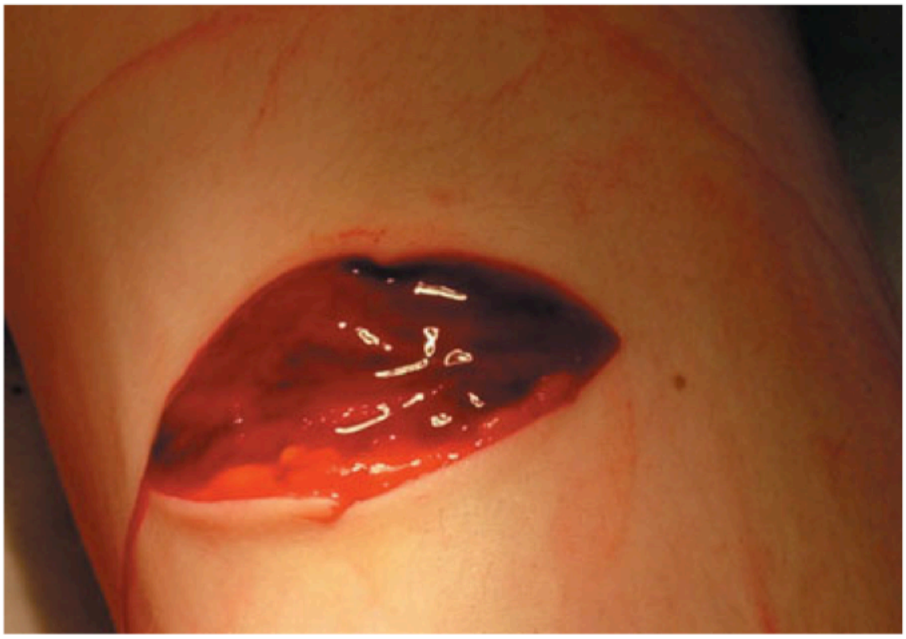

Figure 8.24 Slash-type wound to forearm: wound is wider than it is deep.

Figure 8.26 Multiple hypertrophic scars to left arm and shoulder caused by machete.

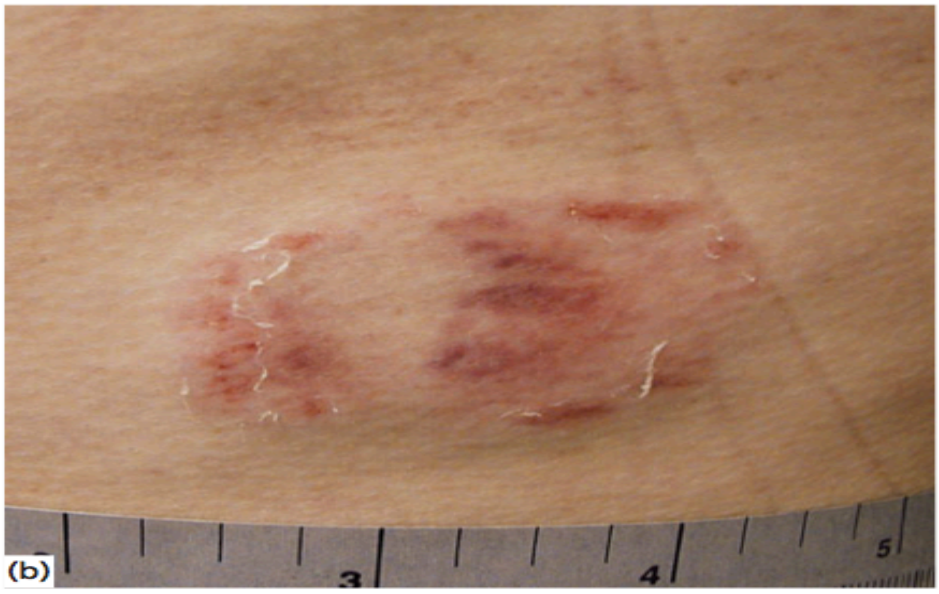

Figure 8.28 Bites. **(a)** Human bite with tissue loss to right ear. **(b)** Bite mark with bruising, skin lifts and teeth marks to chest. **(c)** Bite causing tissue loss to chin no clear teeth marks evident.

Figure 8.27 Typical severe fingernail scratching injuries to face.

Figure 8.29 Defence injuries to right hand caused by knife.

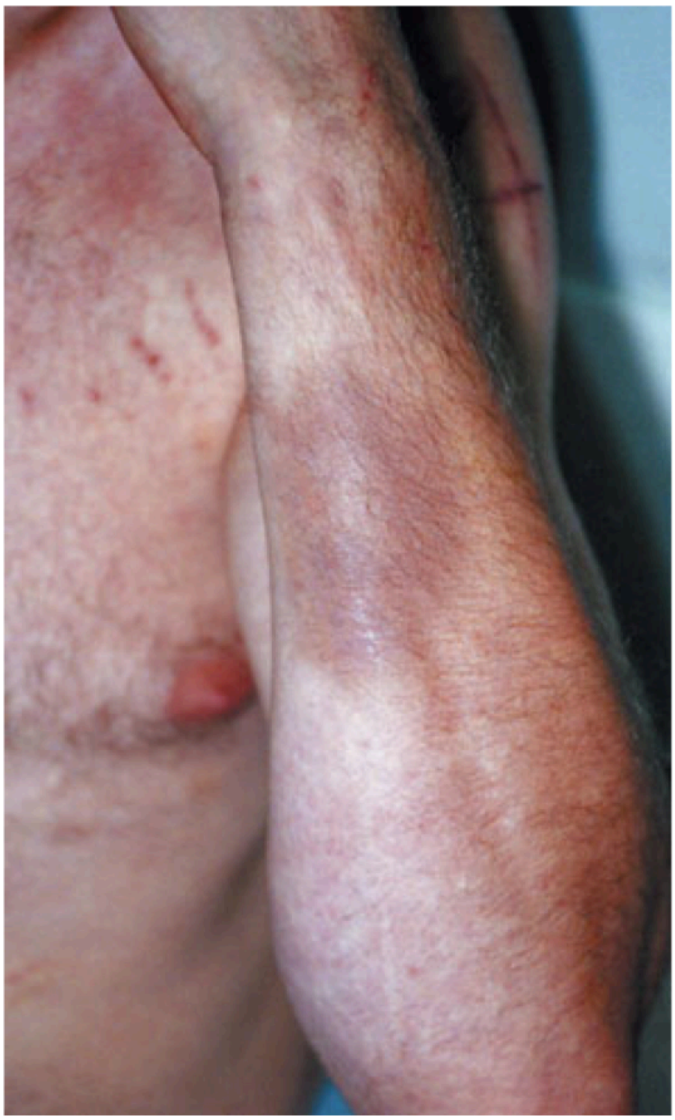

Figure 8.30 Bruising to extensor aspect of left arm – raised to ward off impact from baseball bat.

Figure 8.31 **(a)** Multiple linear burn marks (caused by heated knife blade applied to the skin) – note healed lesions between acute lesions. **(b)** Multiple incised wounds to forearm – note different ages of scars.

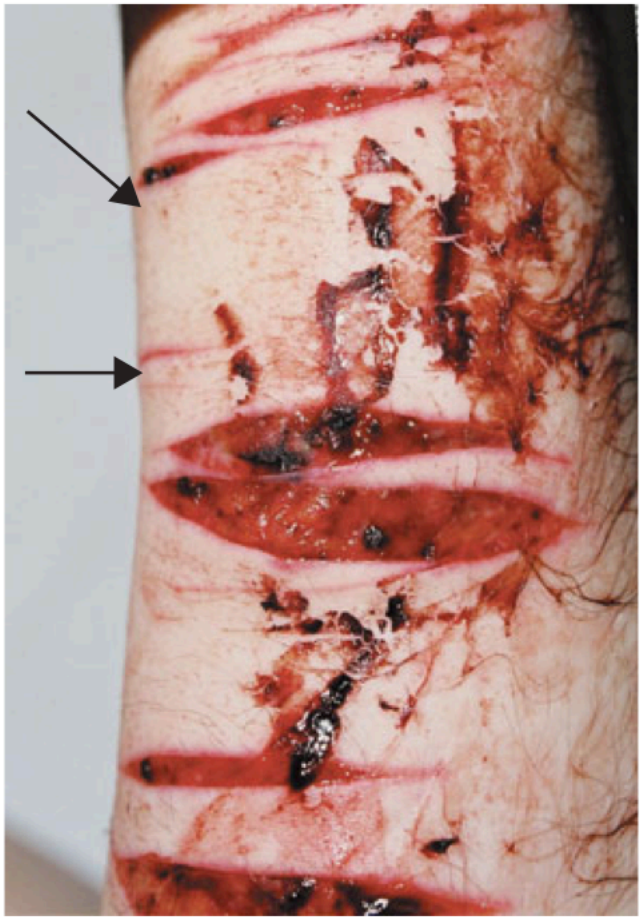

Figure 8.32 Multiple new incised wounds with smaller and more superficial tentative injuries (arrowed).

Figure 8.34 Amputation of right thumb as a form of torture.

Figure 8.35 Visible abnormality subsequent to joint disruption after Palestinian hanging.

Figure 8.33 Bruising to feet caused by repeated blunt impact to feet – falanga.

Figure 8.36 Electrical burns – scarring to scrotum as a result of application of electrodes.

Chapter 9: Regional injuries

Figure 9.1 Scalp laceration caused by a heavy torch. Following shaving of hair from around the injury, the crushed and abraded wound edges can clearly be seen.

Figure 9.3 Depressed skull fracture, with rounded contours, closely replicating the dimensions of a round-headed hammer.

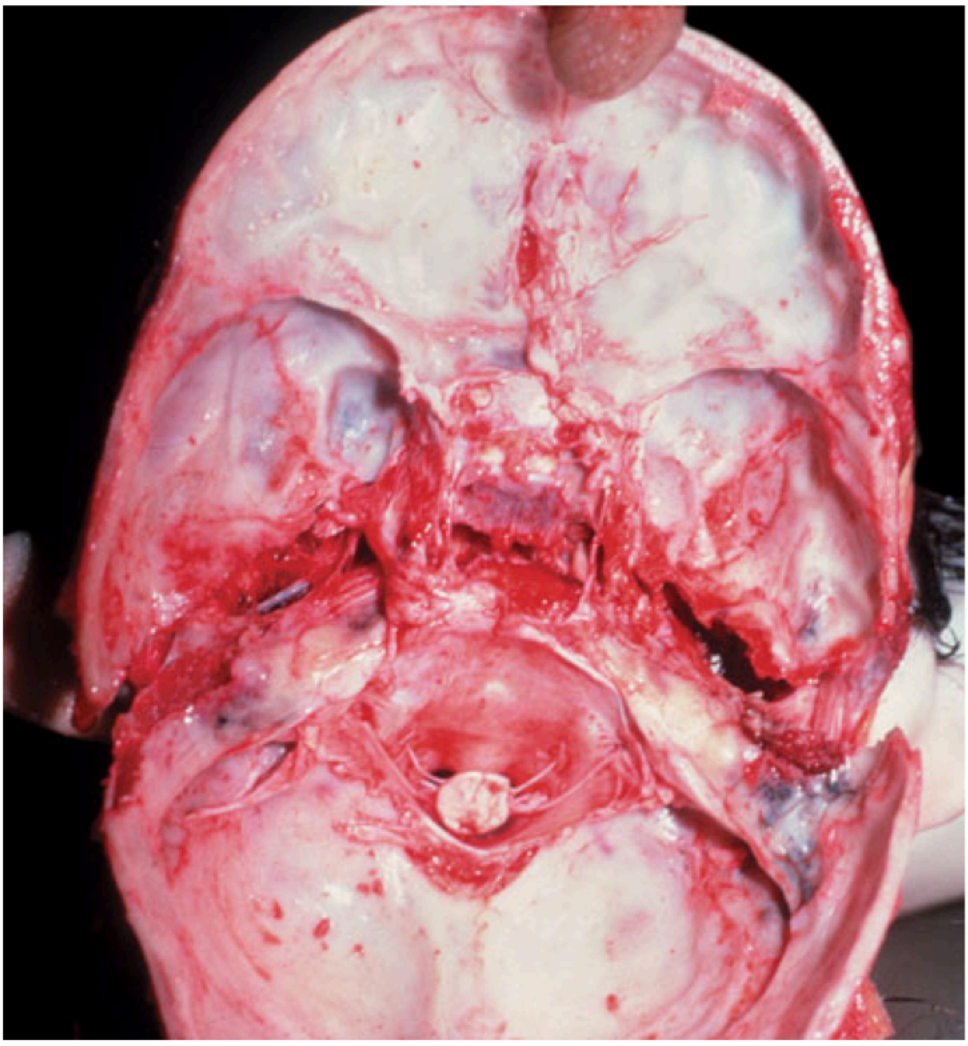

Figure 9.2 A 'hinge fracture' of the skull base caused by impact to the left side of the head after the victim was thrown to the ground, having been hit by a car.

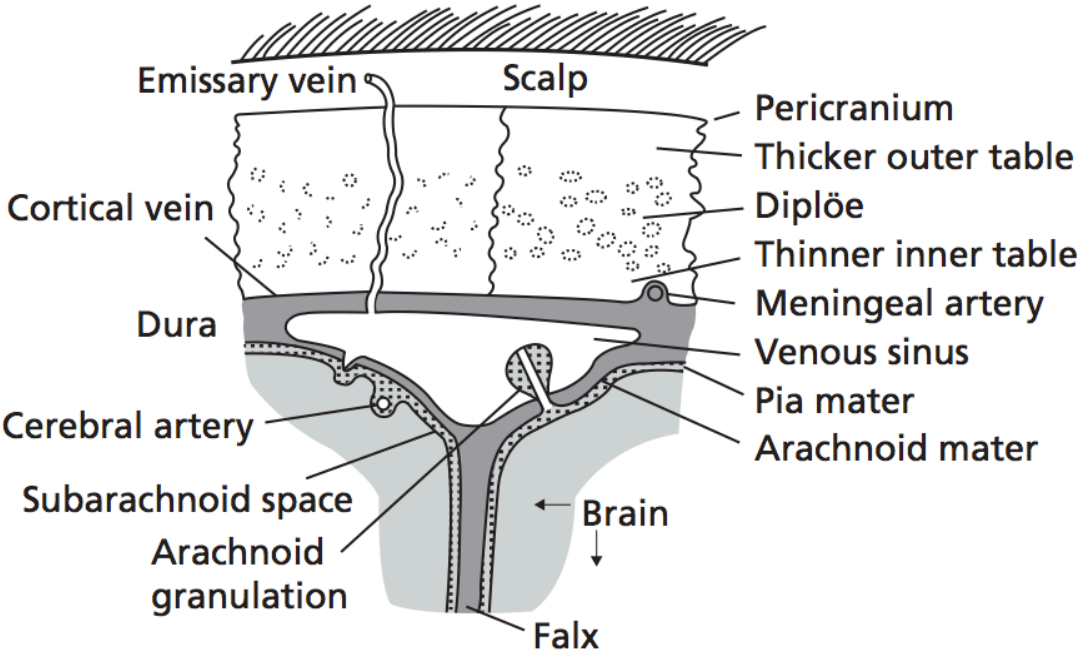

Figure 9.4 Forensic anatomy of the skull and meninges.

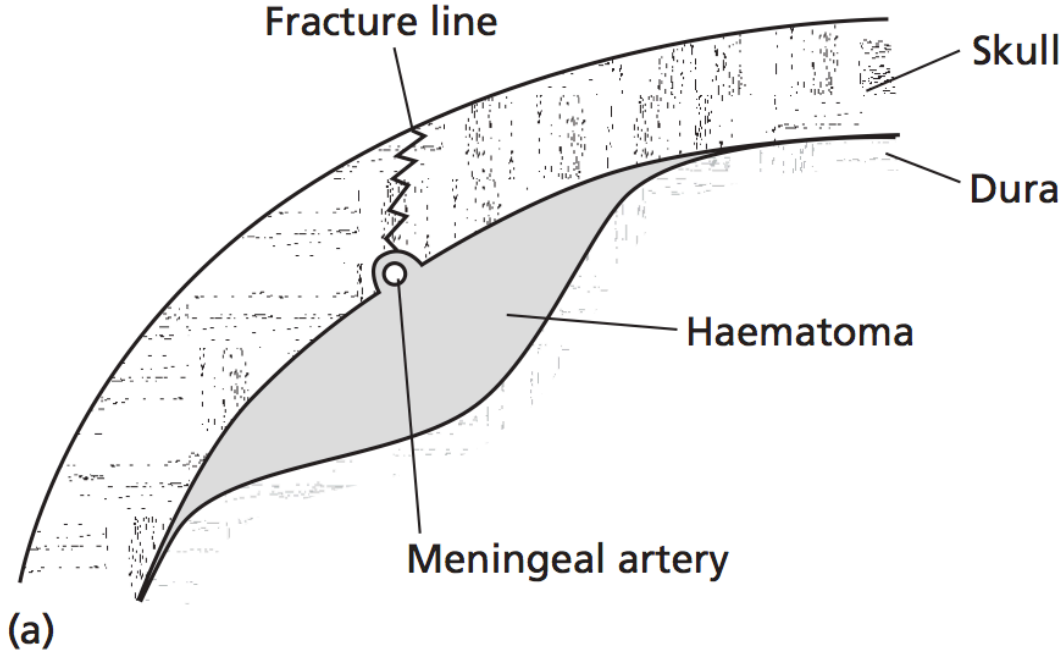

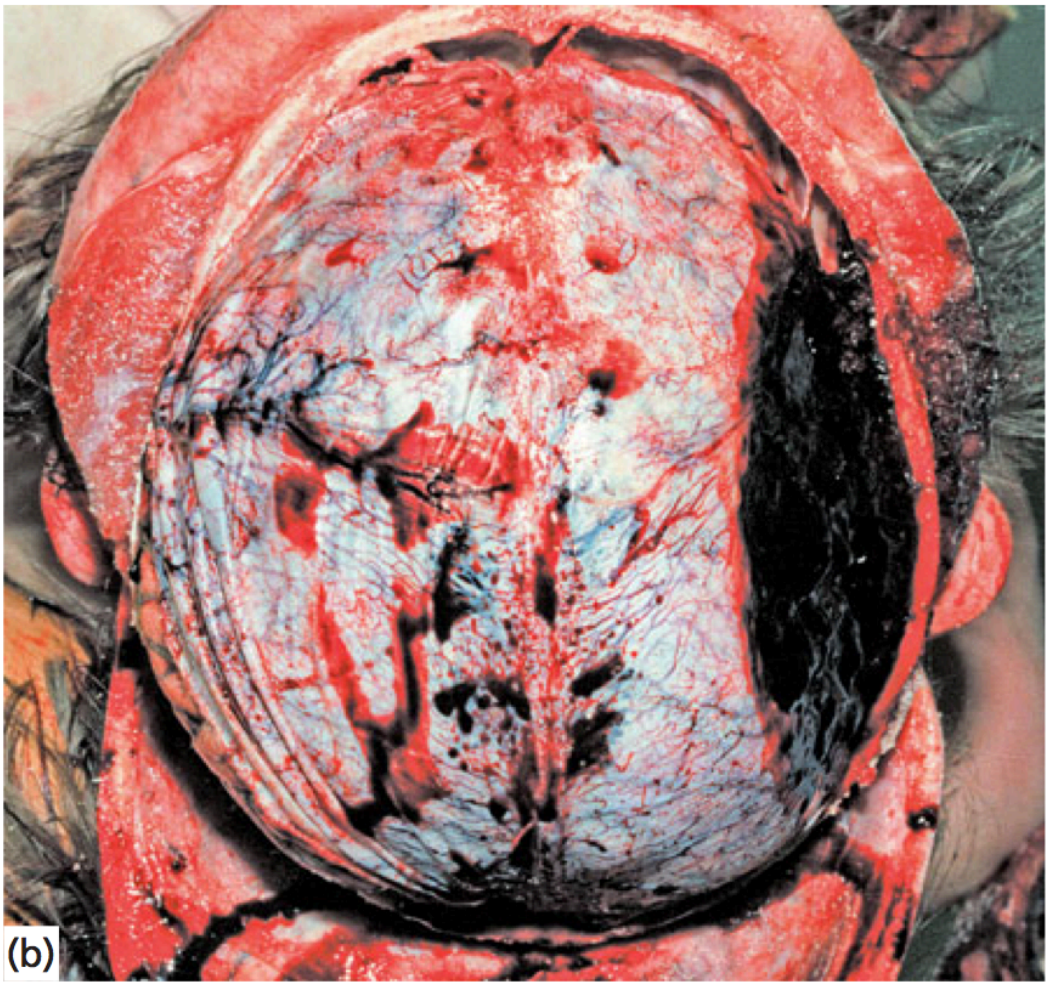

Figure 9.5 Extradural haemorrhage. Schematic representation **(a)** of the formation of an extradural haemorrhage and autopsy appearance **(b)** of a large right-sided, temporoparietal, extradural haemorrhage associated with deep scalp bruising at the site of impact. There was a linear skull fracture on the right passing through the middle meningeal artery.

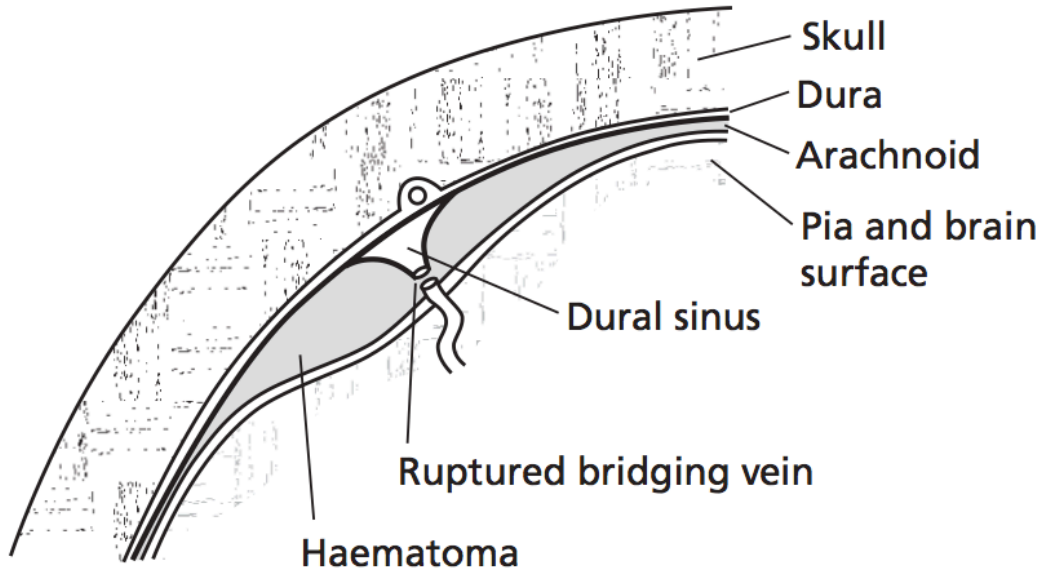

(a)

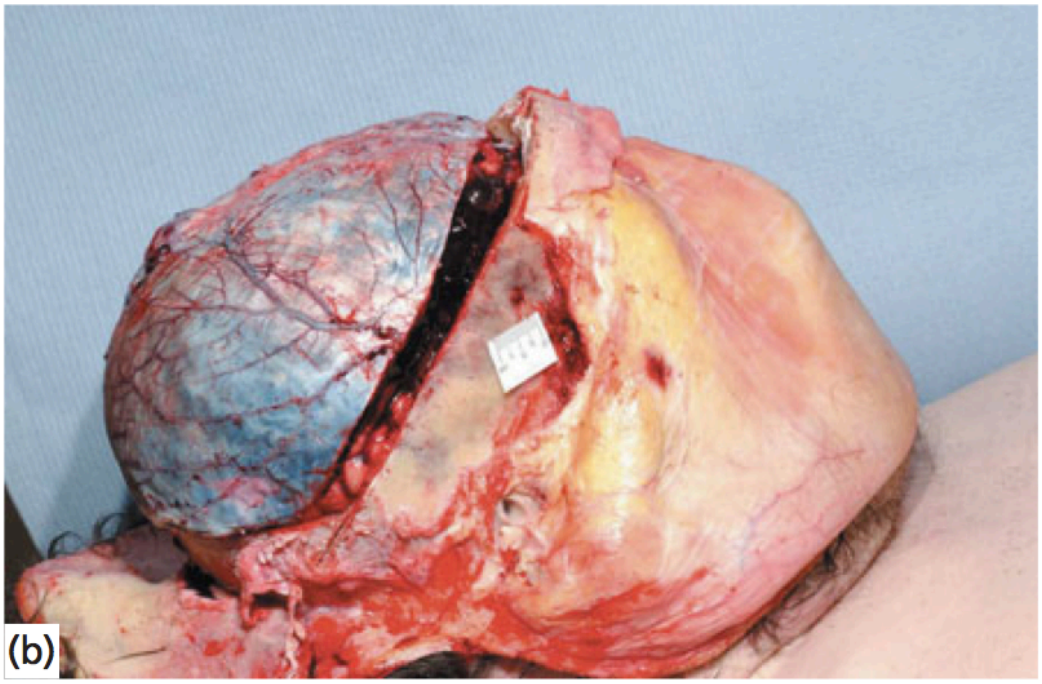

(b)

Figure 9.6 Subdural haemorrhage. Schematic representation of the formation of a subdural haematoma **(a)** and autopsy appearance of an acute right-sided subdural haemorrhage **(b)**.

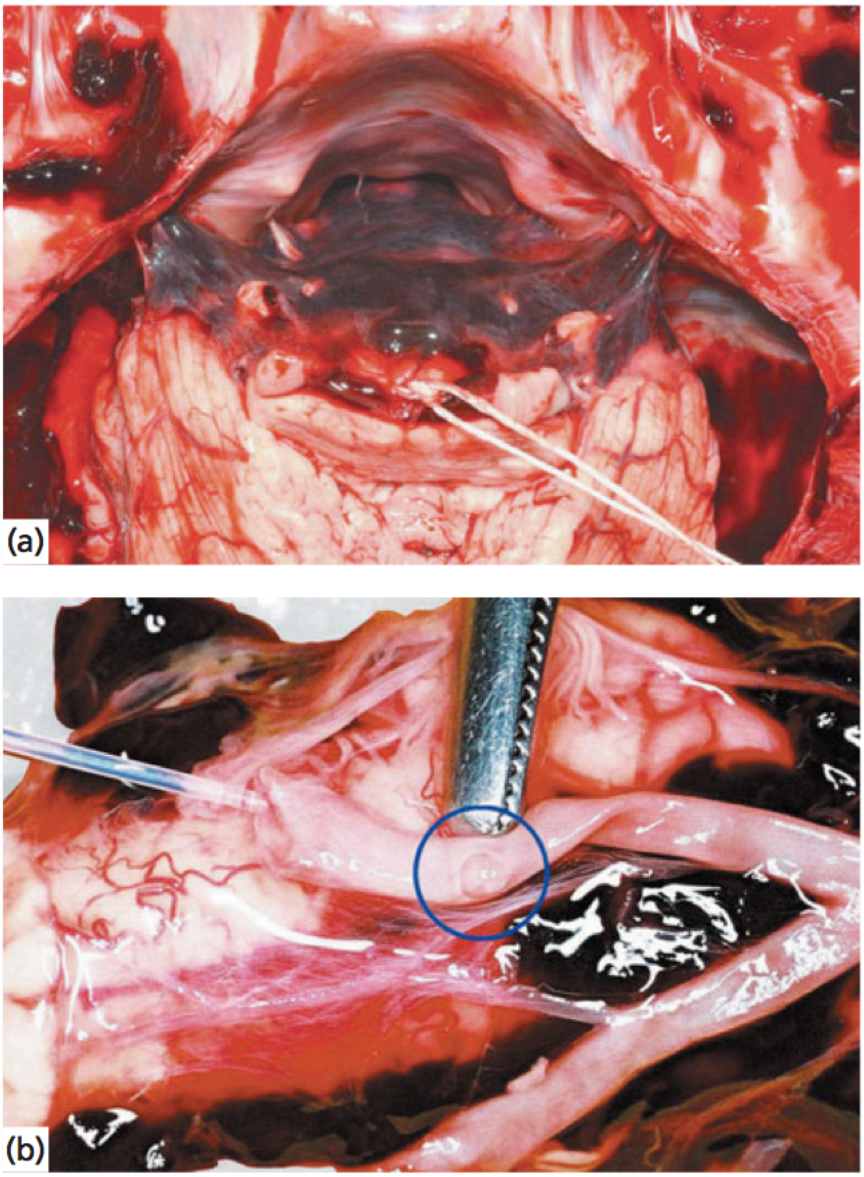

Figure 9.8 Traumatic basal subarachnoid haemorrhage. **(a)** Autopsy appearance of basal subarachnoid haemorrhage, covering the brain-stem, visualized following removal of the cerebral hemispheres and tentorium cerebelli. The basilar artery has been ligated. **(b)** The source of the bleeding is a tear in a vertebral artery, confirmed following visualization of fluid leakage from the cannulated injured vessel.

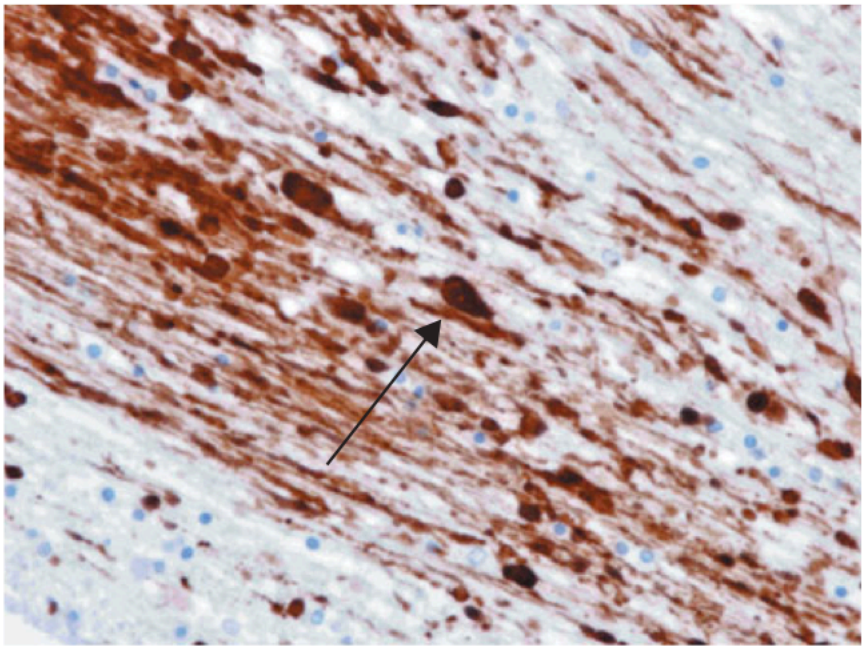

Figure 9.10 Microscopy of axonal injury. The immunohistochemical staining of β-amyloid precursor protein (β-APP) demonstrates axonal injury in white matter (corpus callosum). Discrete axonal swellings and 'axonal retraction bulbs' can be visualized following traumatic brain injury if the injured person survived for some hours after sustaining their head injury.

Figure 9.12 Contrecoup contusions on the under-surface of the brain.

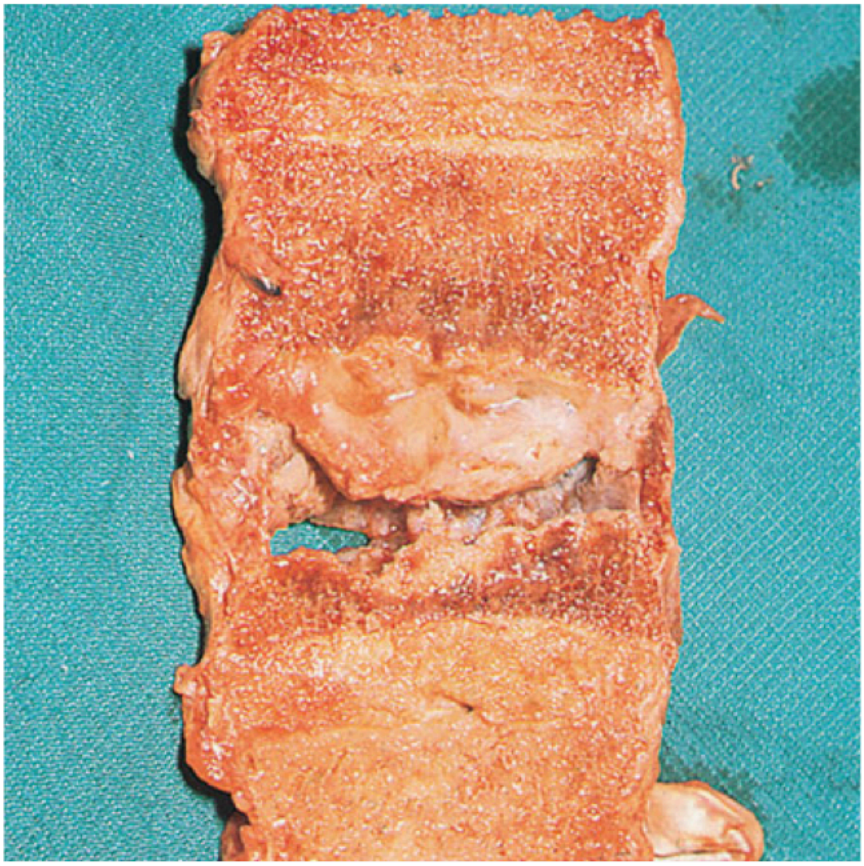

Figure 9.13 Crushed vertebral body as a result of a hyperflexion injury.

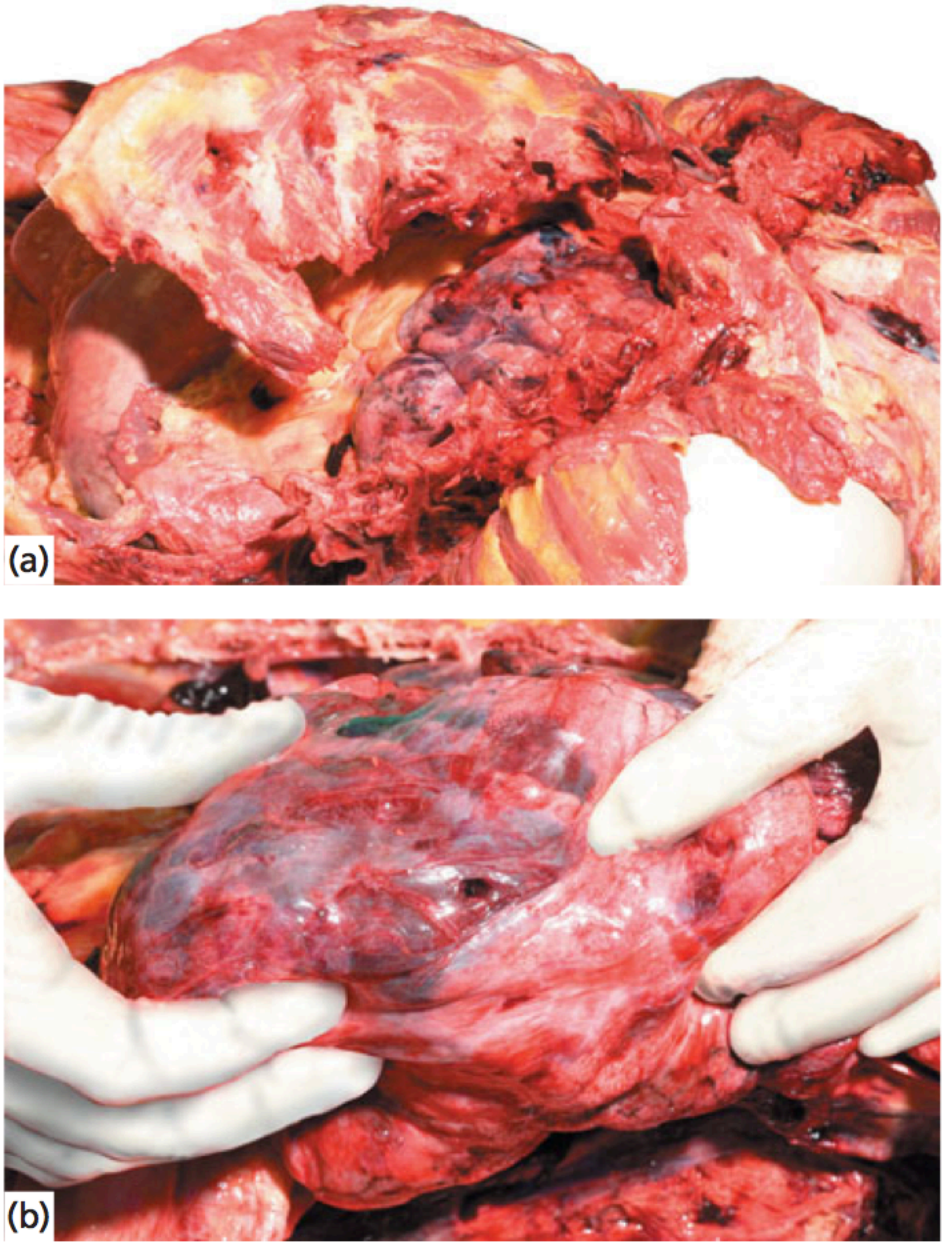

Figure 9.14 Multiple rib fractures **(a)** following a road traffic collision. There were many 'flail' segments and fractured rib ends pierced the underlying lung **(b)**.

Figure 9.15 Mesenteric bruising and laceration following blunt force trauma in a road traffic collision.

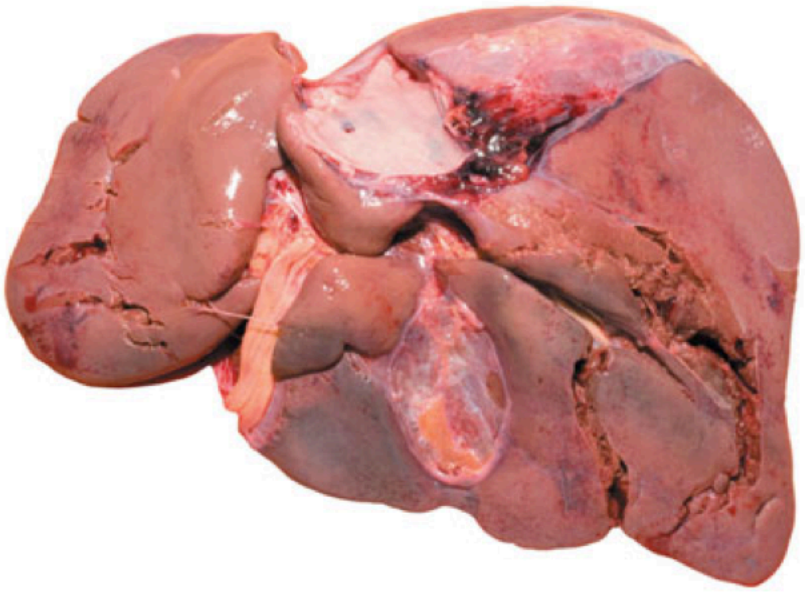

Figure 9.16 Multiple lacerations of the liver following blunt force abdominal trauma in a road traffic collision.

Chapter 10: Ballistic injuries

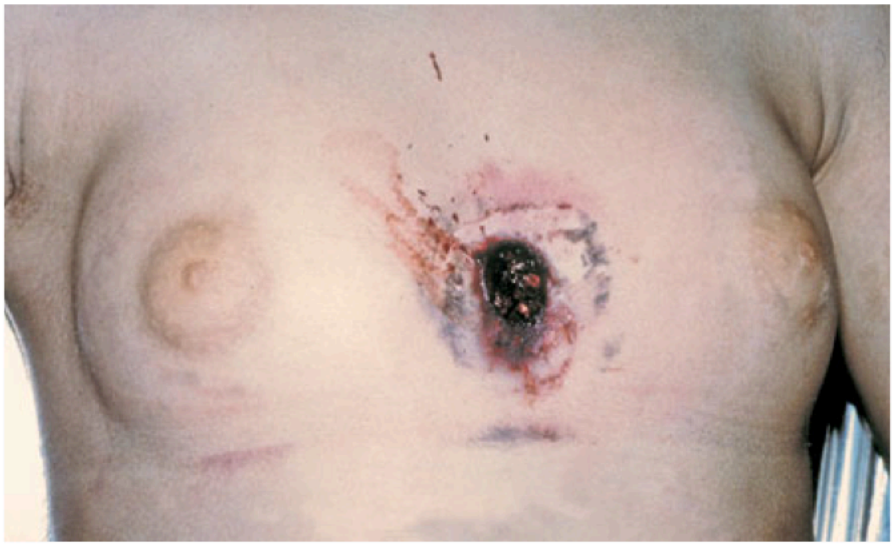

Figure 10.2 Suicidal twelve-bore shotgun entrance wound, with soot soiling. The wound shows the outline of the non-fired muzzle, indicating that the weapon was a double-barrelled shotgun pressed against the skin at discharge.

Figure 10.3 Firm contact entrance wound from a twelve-bore shotgun. Clothing prevented soot soiling, but minor peripheral abrasions were caused by impact of a belt. Gas expansion in the distensible abdomen has prevented skin splitting at the wound edges.

Figure 10.4 Suicidal close range discharge of a twelve-bore shotgun wound to the chest. This wound has torn a large ragged defect in the chest wall and there is soot discoloration at the medial wound edge because of the tangential orientation of the discharge.

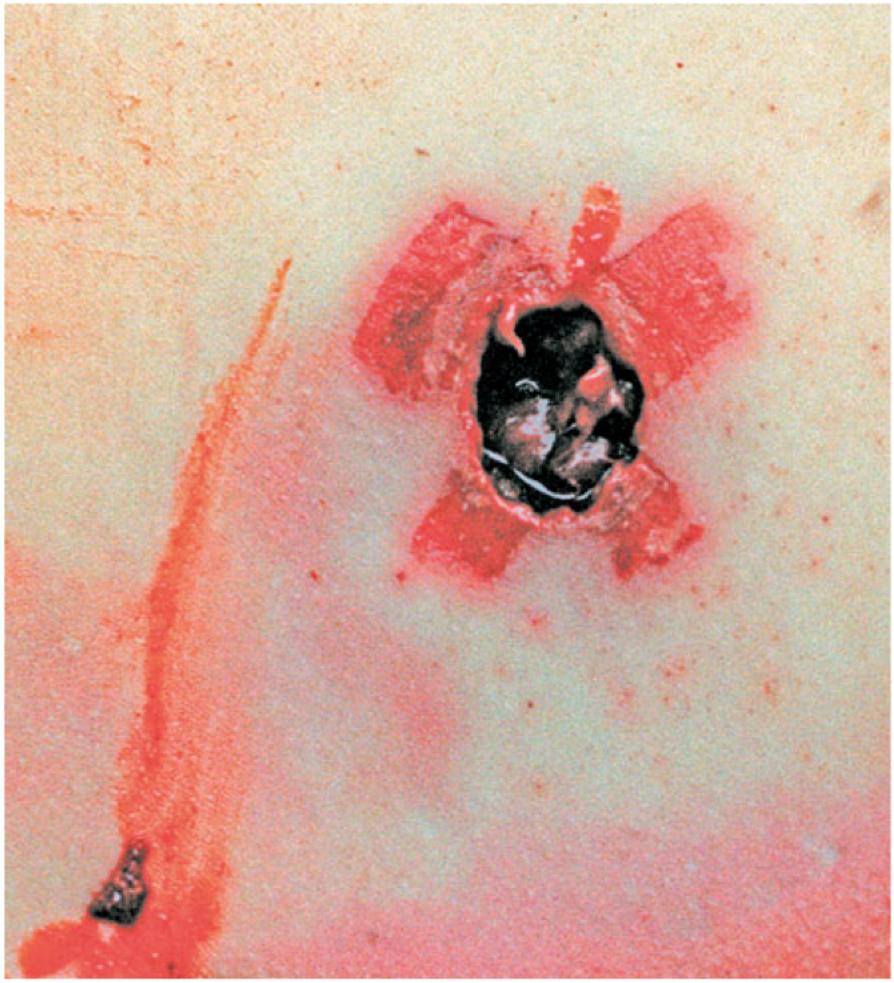

Figure 10.5 Abraded bruise surrounding an intermediate-range homicidal shotgun entrance wound, caused by impact against the skin from the opening up of the plastic pellet container. Note the scalloping of the wound edges.

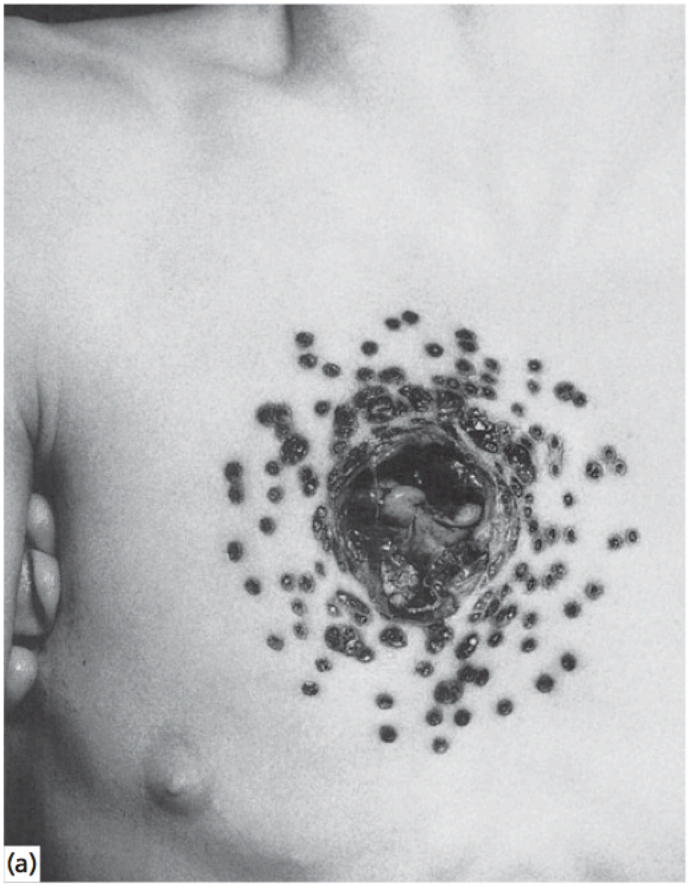

Figure 10.6 **(a)** Distant-range shotgun entrance wound, with a central hole surrounded by peripheral satellite pellet holes. This wound was caused by discharge from approximately 4 m; measurement of shot-spread can be compared with that created from test-firing the suspect weapon and ammunition to provide a more accurate assessment of range of fire. **(b)** Shotgun pellet injury to skin from discharge about 12 m away

Figure 10.7 Suicidal twelve-bore shotgun entrance wound in a 'site of election' under the chin. The circular soot discoloration on the skin surface indicates a very close (or even 'loose' contact) discharge. Note the extensive destruction reflecting the explosive effect of shotgun discharges to the head.

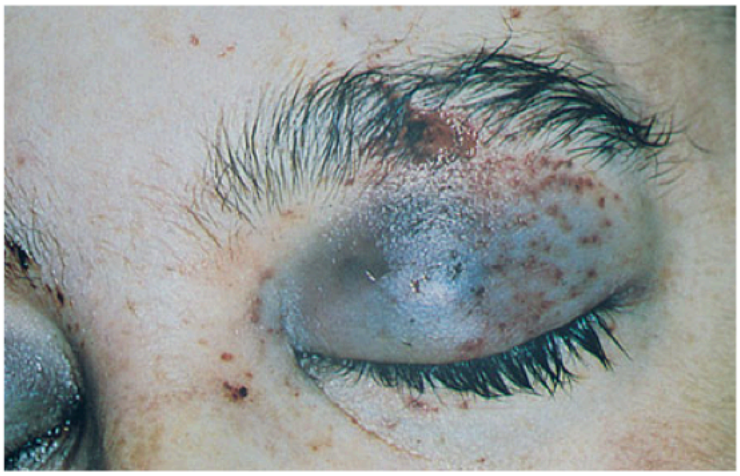

Figure 10.8 Close-range gunshot entrance wound from a pistol, with powder tattooing on the adjacent skin. The eye is blackened as a result of bleeding 'tracking' down from fracturing of the anterior cranial fossa in the skull base.

Figure 10.9 Suicidal contact gunshot entrance wound to the temple. The skin is burnt and split because of the effects of the discharge products.

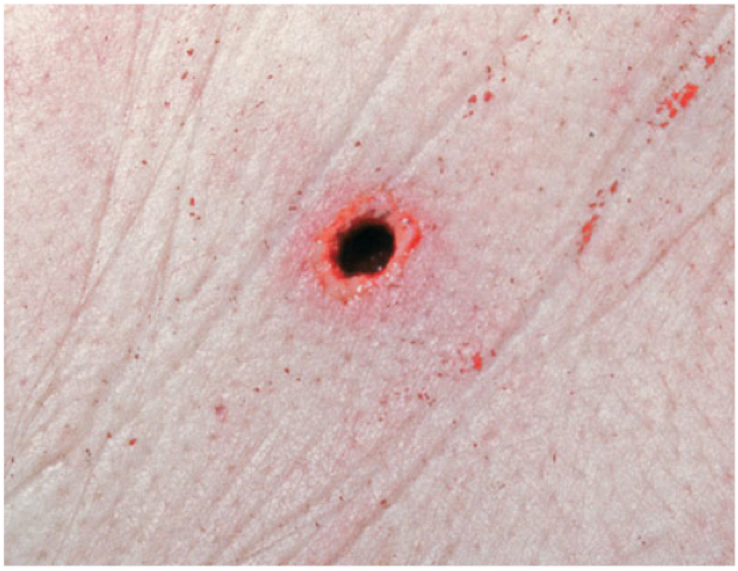

Figure 10.10 Circular distant gunshot entrance wound from a rifle bullet. There is no associated soot soiling or burning of the wound edges, with only minimal marginal abrasion and bruising.

Figure 10.11 Typical exit wound with everted, split edges, with no soiling of the surrounding skin.

Figure 10.12 Multiple abrasions and lacerations caused by flying debris projected in a bomb blast.

Figure 10.13 Massive disruption of the body of an individual who had constructed an explosive device.

Chapter 11: Use of force and restraint

Figure 11.1 Scleral haemorrhage 2 hours after neck compression in a restraint setting.

Figure 11.2 Handcuff injuries. **(a)** Imprint of handcuff following tight, prolonged application; **(b)** bruise, abrasion, laceration and underlying ulnar fracture following struggle after handcuff applied.

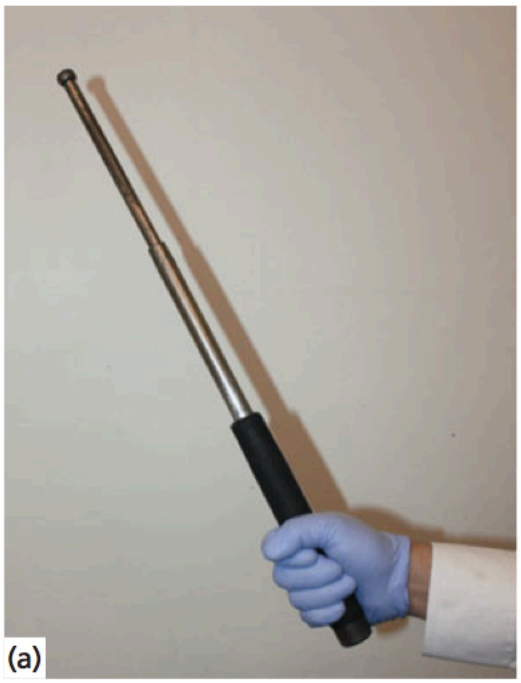

Figure 11.3 ASP baton. **(a)** Fully extended and **(b)** non-extended expandable.

Figure 11.4 Baton imprint.

Figure 11.5 Example of CS spray containers.

Figure 11.7 Bean bag round.

Figure 11.6 Examples of baton rounds.

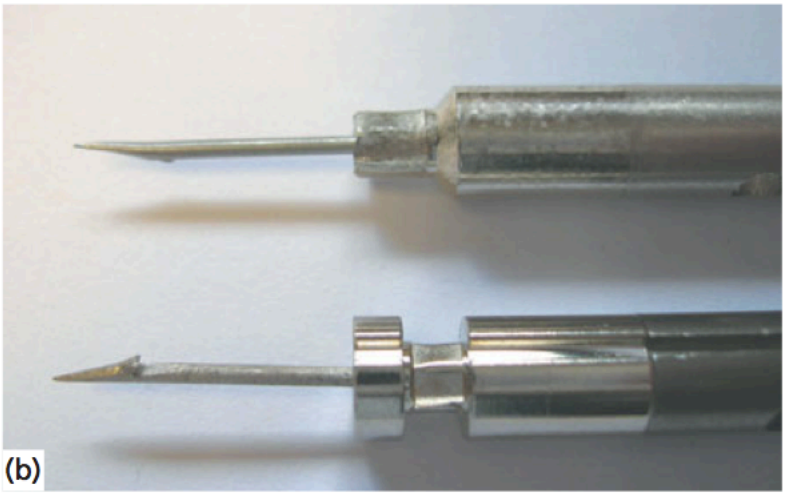

Figure 11.8 **(a)** Taser® X26™ and **(b)** barbs.

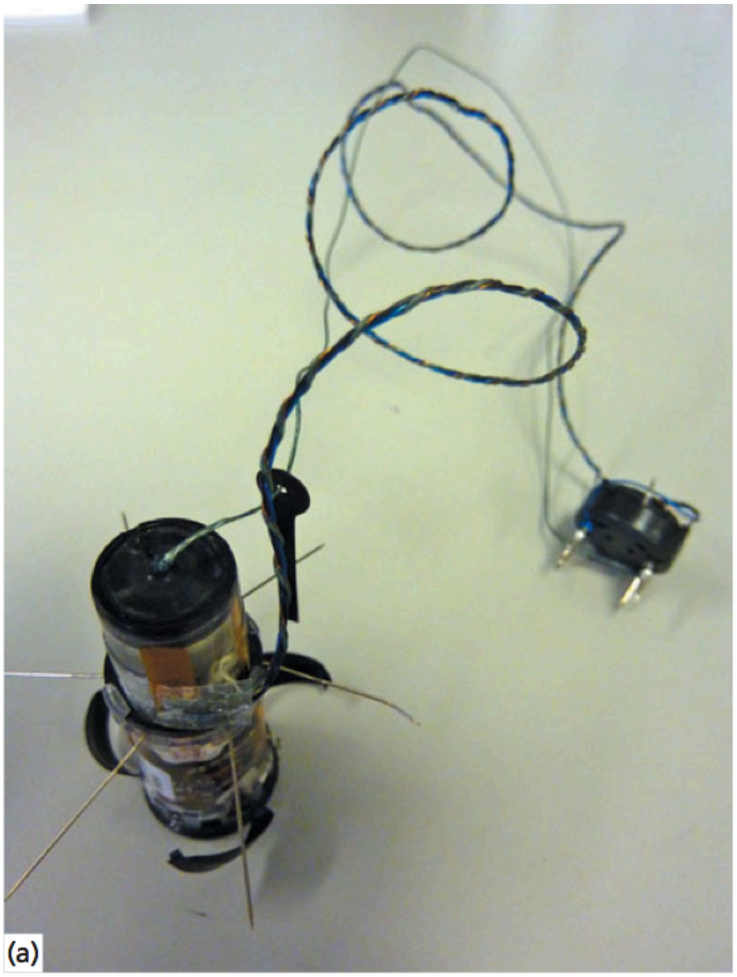

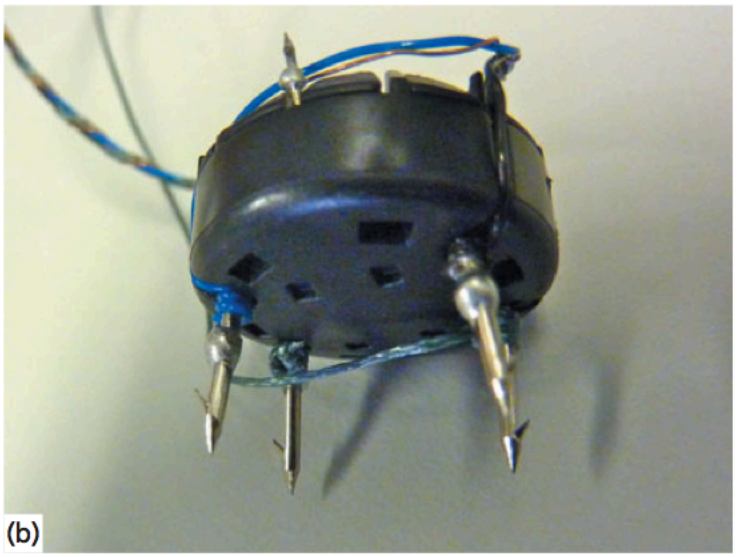

Figure 11.9 **(a)** Taser® XREP™ contact device and **(b)** projectile.

Chapter 13: Child assault and protection

Figure 13.3 Scar caused by application of heated cutlery handle to lower limb.

Figure 13.1 Non-abusive bruising.

Figure 13.2 Inflicted injury-finger marks to neck from slap with hand by non-accidental injury (NAI).

Chapter 14: Transportation medicine

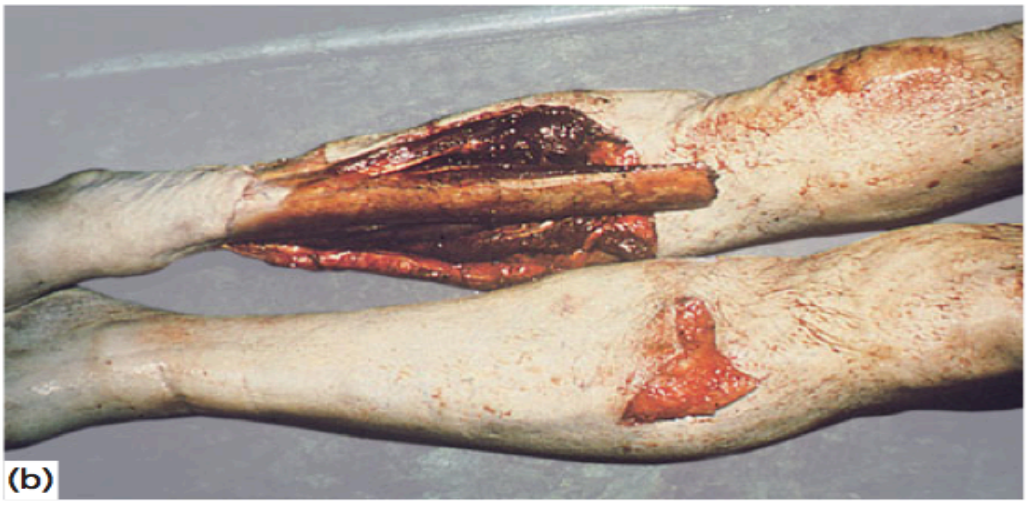

Figure 14.1 **(a)** A pedestrian struck by the front of a car may be projected forwards or lifted onto the vehicle; **(b)** 'bumper injuries' including a compound fracture of the right leg, and laceration of the left knee, probably following primary impact to this pedestrian's right leg.

Figure 14.4 Intradermal bruising reflecting the pattern of a vehicle tyre tread. Note that the bruising is in the 'valleys' and not the 'hills' in the tread. Scaled photographic documentation of such a patterned injury will allow future comparisons to be made between it and the tread pattern of a suspect vehicle.

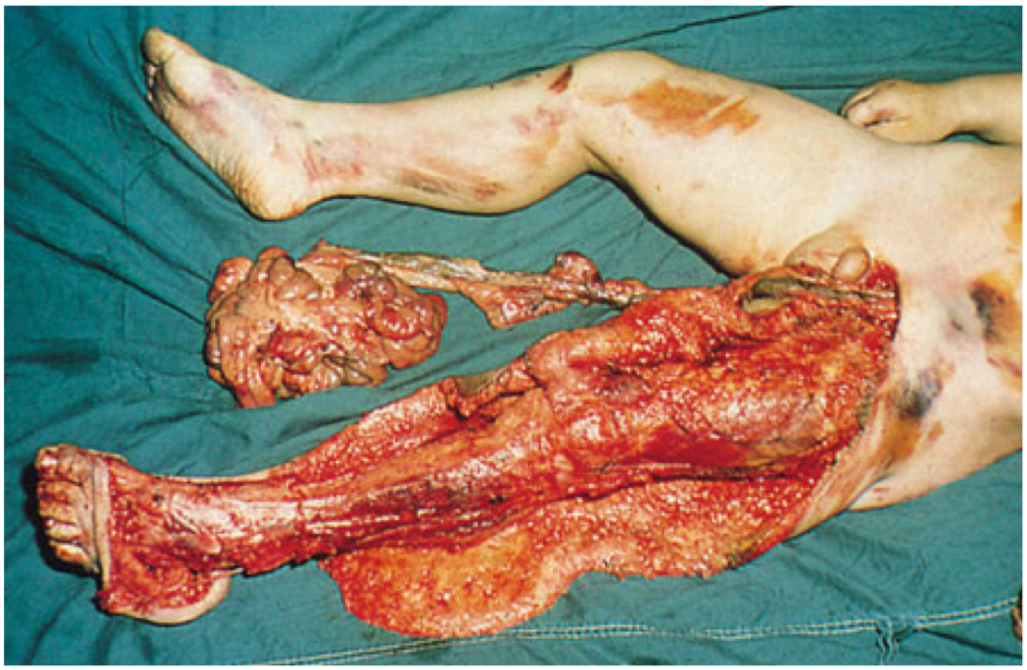

Figure 14.3 Pedestrian leg injury from a rotating wheel resulting in 'flaying' of the skin.

Figure 14.6 Facial injuries from shattered windscreen glass in an unrestrained driver. The toughened glass breaks into small fragments, which produce characteristic ‘sparrow foot’ marks. The forehead laceration was made by the windscreen rim.

Figure 14.7 Deceleration-related thoracic aortic transection following a road traffic collision. The typical site for deceleration aortic injury is just distal to the origin of the left subclavian artery.

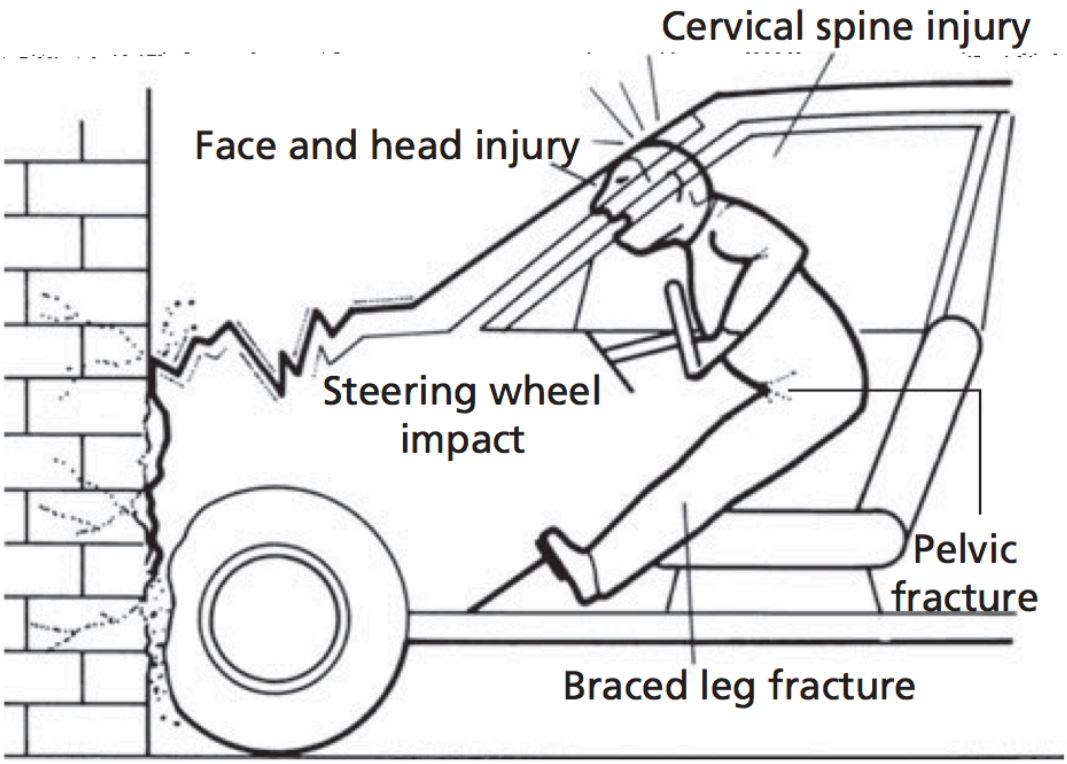

Figure 14.5 Major points of injury to an unrestrained driver of a vehicle in deceleration impact.

Figure 14.8 Extensive ‘brush’ abrasion of the left flank in a motor cyclist thrown across a rough surface.

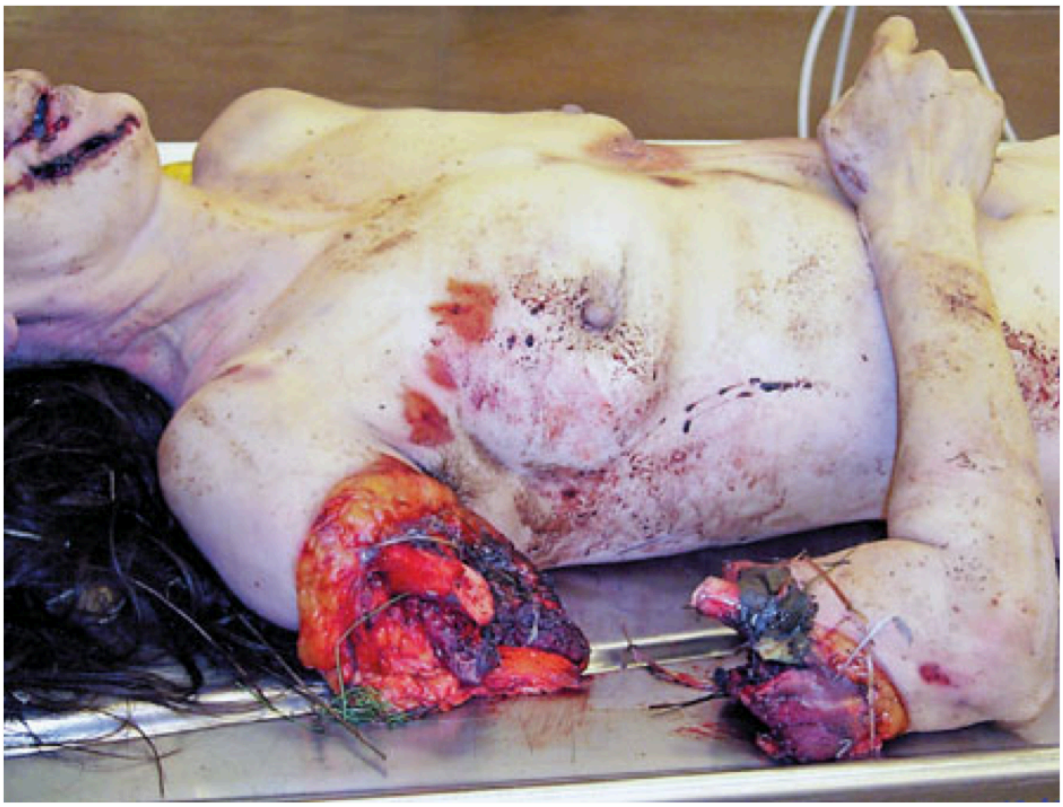

Figure 14.9 Amputation of the right arm and bruising of the face and chest in a pedestrian struck by a passing train.

Figure 14.10 Abrasion of neck caused by mainsheet during uncontrolled gybe.

Chapter 15: Asphyxia

Figure 15.1 **(a)** Examples of the causes of mechanical asphyxia. **(b)** Grip marks to the neck and jaw following attempted manual strangulation. **(c)** Ligature mark after attempted garrotting - note congestion ('tide mark') above double ligature.

Figure 15.2 Petechial (and more confluent) haemorrhages in the facial skin and conjunctivae following manual strangulation.

Figure 15.3 Tardieu spots (subpleural petechial haemorrhages) following manual strangulation. These are no longer considered to be specific for asphyxia.

Table 15.1 Examples of 'asphyxial' conditions

Underlying cause of death	Name
Lack of oxygen in the inspired air	Suffocation
Blockage of the external orifices	Suffocation/smothering
Blockage of the internal airways by obstruction	Gagging/choking
Blockage of the internal airways by external pressure	Strangulation/hanging
Restriction of chest movement	Traumatic asphyxia
Failure of oxygen transportation	(For example carbon monoxide poisoning)
Failure of oxygen utilization	(For example cyanide poisoning)

Figure 15.6 Surface injuries on the neck and jaw in manual strangulation. Note multiple bruises and abrasions; some of these injuries are caused by the victim trying to release the grip of the assailant.

Figure 15.7 Ligature mark from a nylon scarf. Although the fabric was broad, tight stretching of the fabric resulted in a well-defined linear 'band' that could be mistaken for that made by a cord or wire.

Figure 15.8 Layered *in situ* dissection of the anterior neck structures is essential in order to evaluate injuries following pressure to the neck. Such dissection must be carried out following 'drainage' or 'decompression' of the blood vessels in the neck to avoid artefactual haemorrhage.

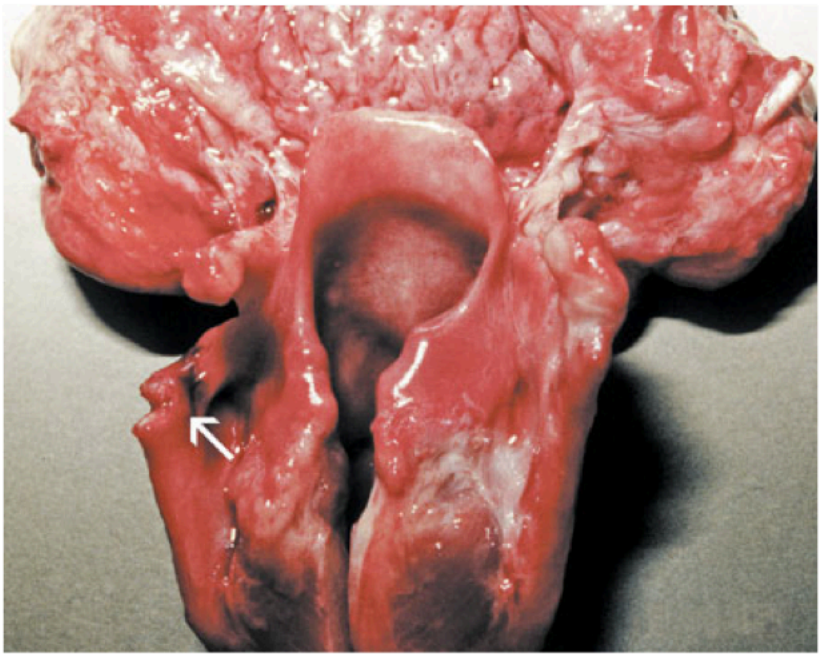

Figure 15.9 Fracture of the left superior horn of the thyroid cartilage following strangulation.

Figure 15.10 Suicidal hanging: the rope rises to a point, leaving a gap in the ligature mark – the suspension point – on the neck.

Figure 15.11 A deep furrowed ligature mark under the chin, and rising to the back of the neck, in hanging. Note the spiral weave pattern visible in the parchmented mark.

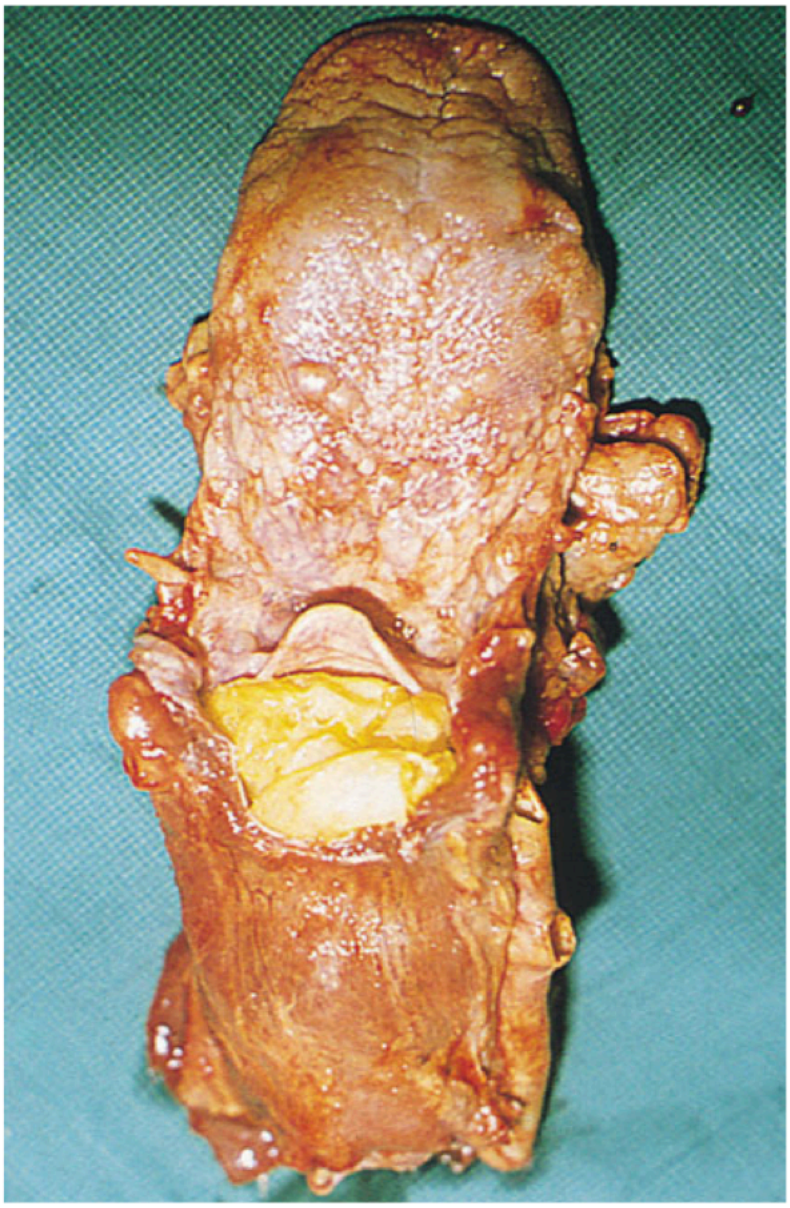

Figure 15.12 Impaction of food in the larynx – café coronary.

(a)

(b)

Figure 15.13 Traumatic asphyxiation in the workplace: **(a)** there is gross congestion of the head and face, with petechiae following burial, up to the axillae, in an avalanche of iron ore, and **(b)** gross conjunctival haemorrhages following chest compression by ash.

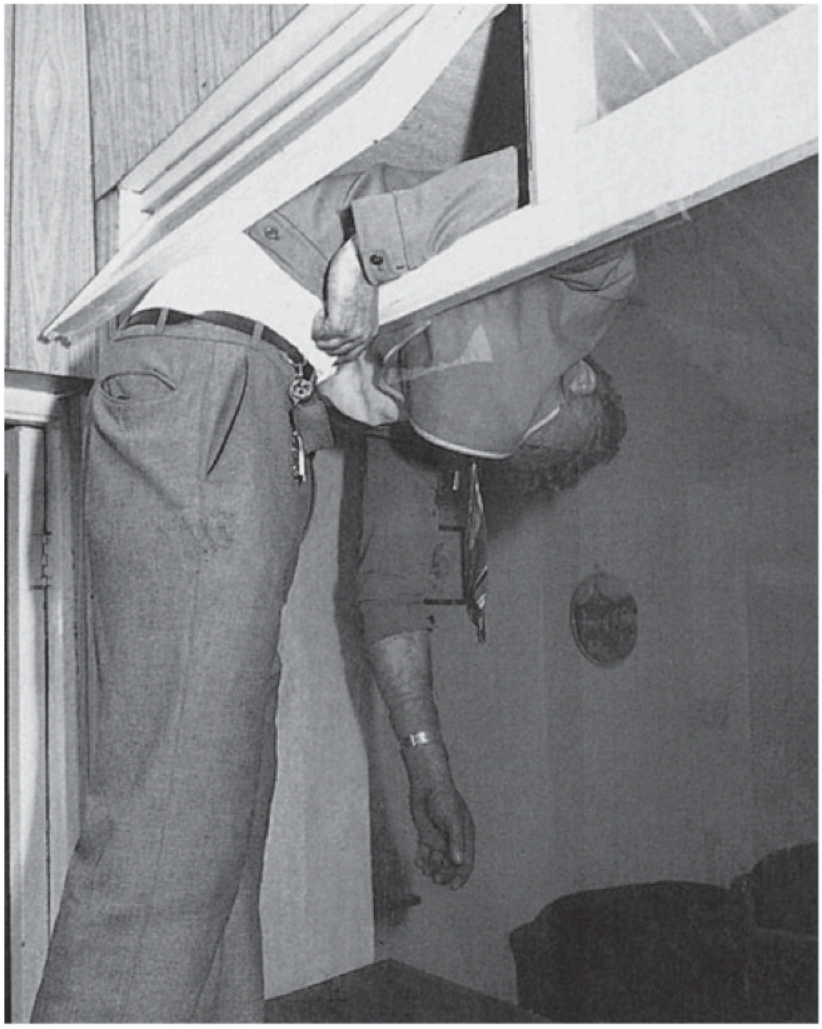

Figure 15.14 Postural asphyxiation. This intoxicated individual slipped and fell from a window sill while trying to climb through a fanlight window. He became wedged and could not make sufficient respiratory movements. Facial (and left arm) congestion and hypostasis is present.

Figure 15.15 Suicidal plastic bag asphyxia. Suffocation by plastic bag often leaves no autopsy asphyxial signs, and removal of the bag by another individual prior to autopsy would cause significant interpretation problems.

Chapter 16: Immersion and drowning

Figure 16.2 Peeling of the epidermis from the foot (degloving) following a few weeks of immersion.

Figure 16.1 'Washer woman's hands'. Waterlogged skin after 1 week of immersion in a cold climate.

Figure 16.3 Post-mortem injuries to the back of the hand in a body recovered from a shallow river. Such injuries are likely to have been caused by contact against the river bed.

Figure 16.4 Post-mortem injuries caused by marine creature predation. This body was recovered from the sea and the circular skin defects are likely to have been caused by crustaceans such as crabs.

Figure 16.5 Frothy fluid exuding from the mouth following drowning.

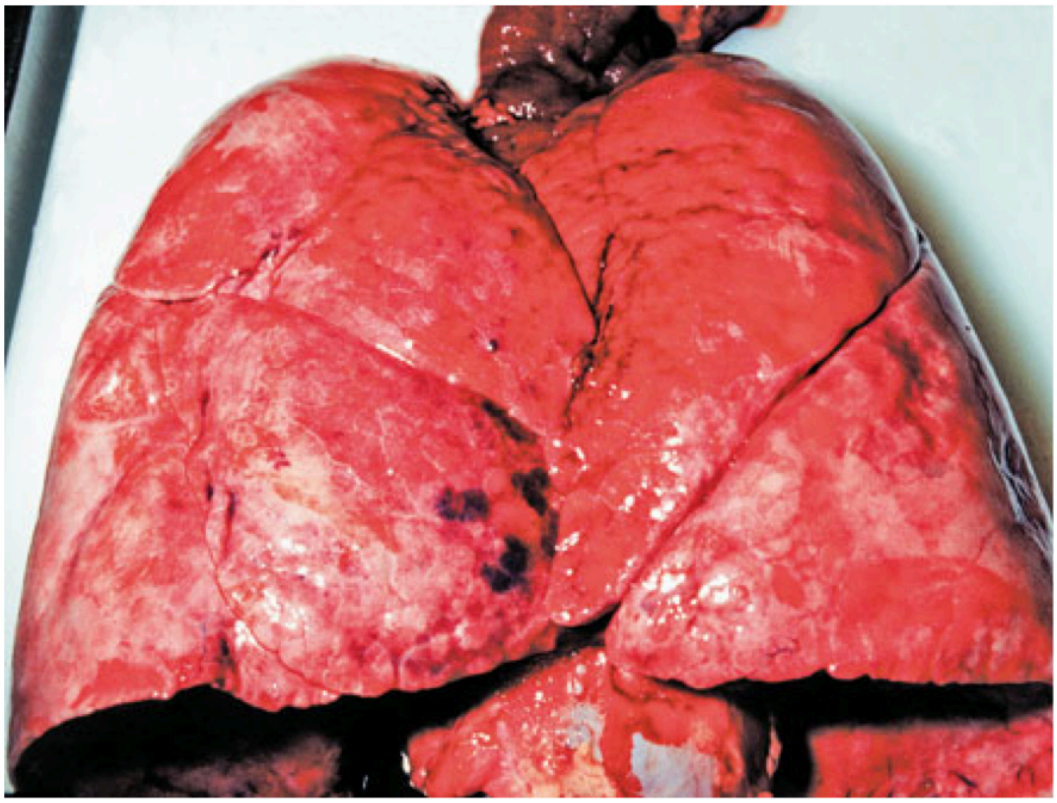

Figure 16.6 Emphysema aquosum following drowning. The lungs are hyperinflated, crossing the midline and obscuring the pericardial sac. There are subpleural haemorrhages in the right lung middle lobe (Paultauf's spots).

Chapter 17: Heat, cold, end electrical trauma

Figure 17.1 The extensiveness of burns on a body recovered from a fire may be varied. This individual had second and third degree burns after dousing himself with petrol before setting himself on fire (self-immolation). Note the molten and singed hair.

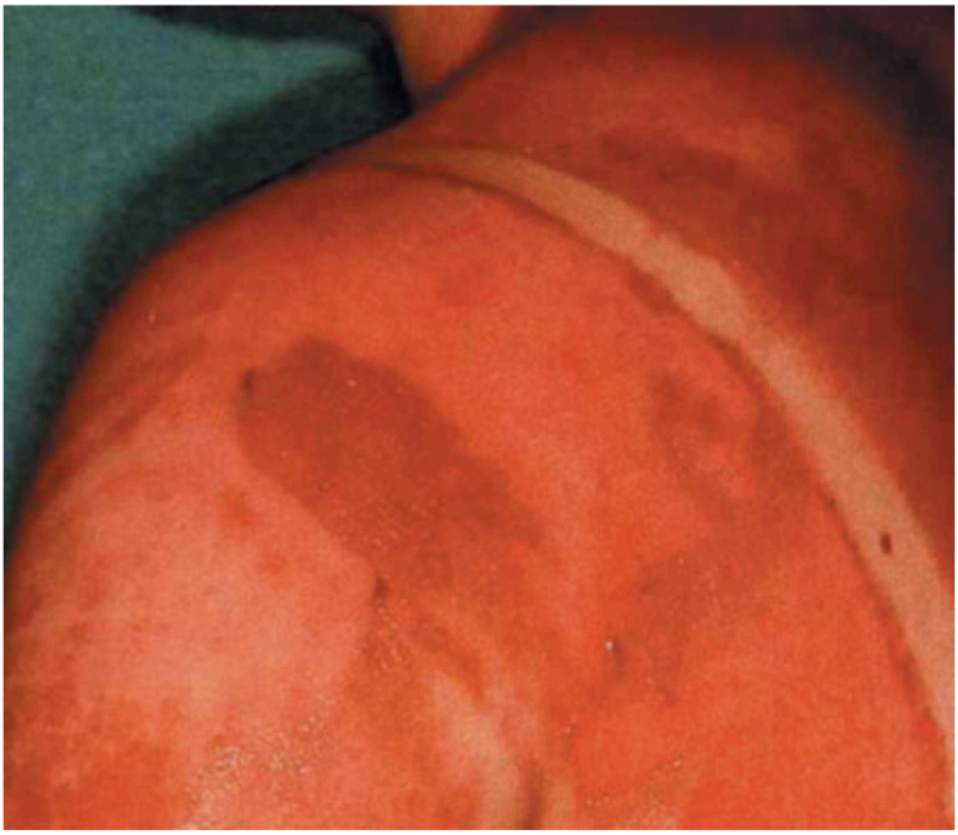

Figure 17.3

Figure 17.4 Pattern of scalding from running water.

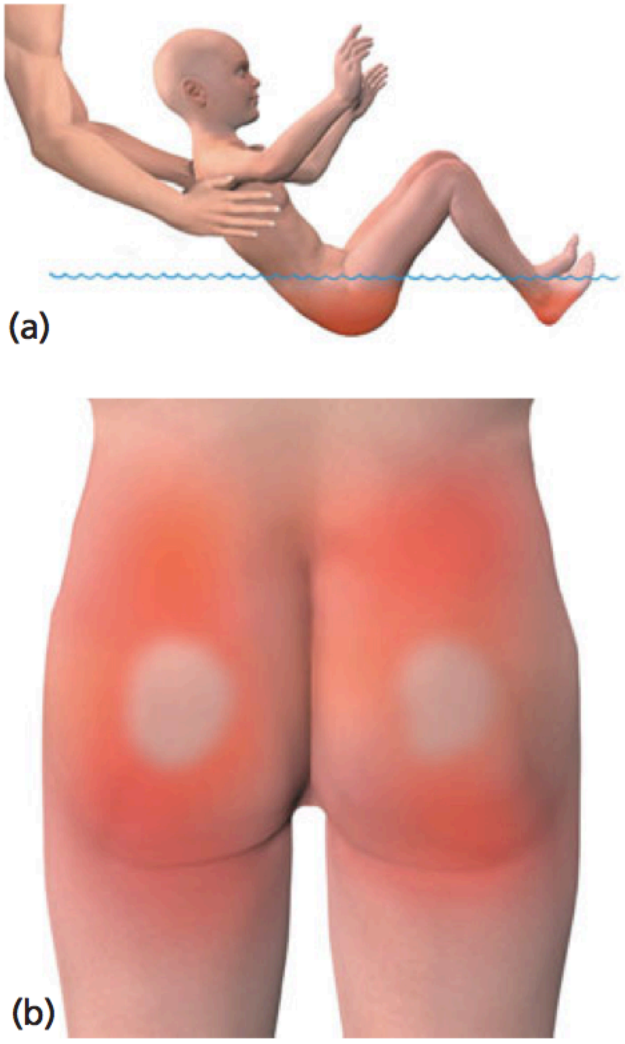

Figure 17.5 Pattern of scalding from forced immersion in a hot bath. Note the clear demarcation between scalded and uninjured skin representing the fluid level of the bath. Sparing of skin on the buttocks reflects firm contact between those parts and the base of the bath.

Figure 17.6 Charred body at the scene of a fire showing the 'pugilist attitude' and post-mortem skin splits on the chest. Extreme care must be taken to preserve the teeth in such cases, in order to assist identification of the deceased.

Figure 17.7 The finding of a body in a burnt-out car should always be treated with suspicion. Carboxyhaemoglobin levels may be low in rapid flash petrol fires leading to difficulties in assessing vitality at the time of the fire.

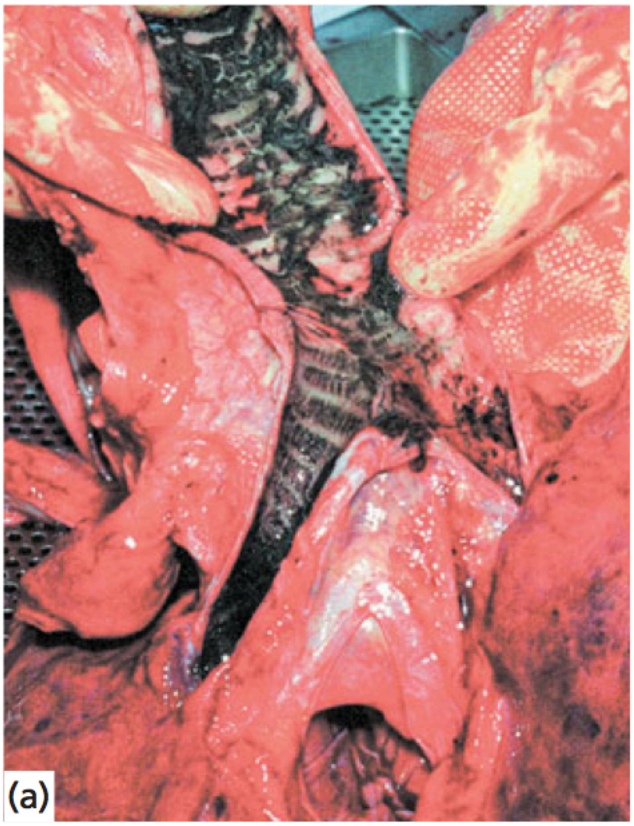
(a)

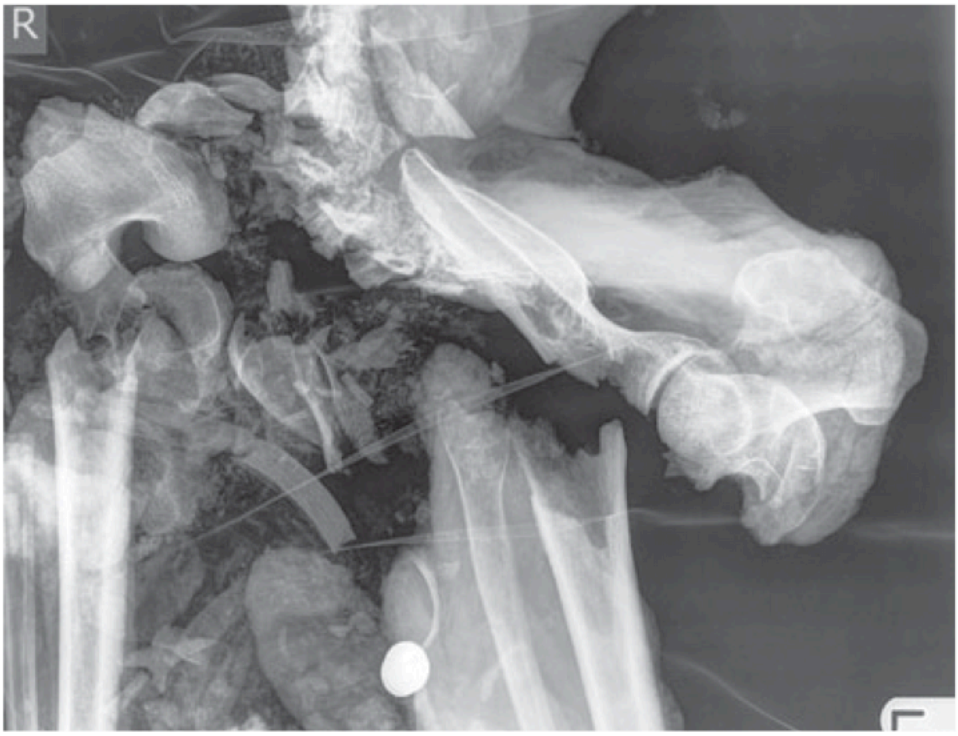

Figure 17.8 Radiography of charred remains is recommended in order to look for projectiles. These fragmented burnt remains include part of a disposable lighter.

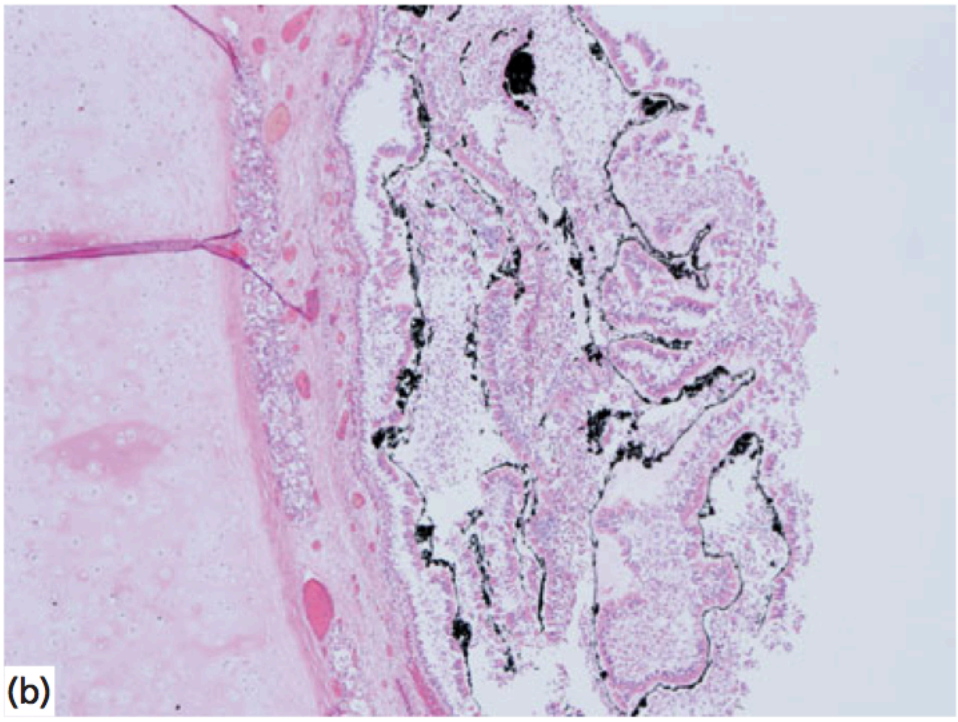

Figure 17.9 Pathological evidence of vitality at the time of the fire. Soot staining following inhalation of the combustion products of fire is clearly visible to the 'naked eye' in this trachea **(a)**, and such a finding can be confirmed under the microscope **(b)**.

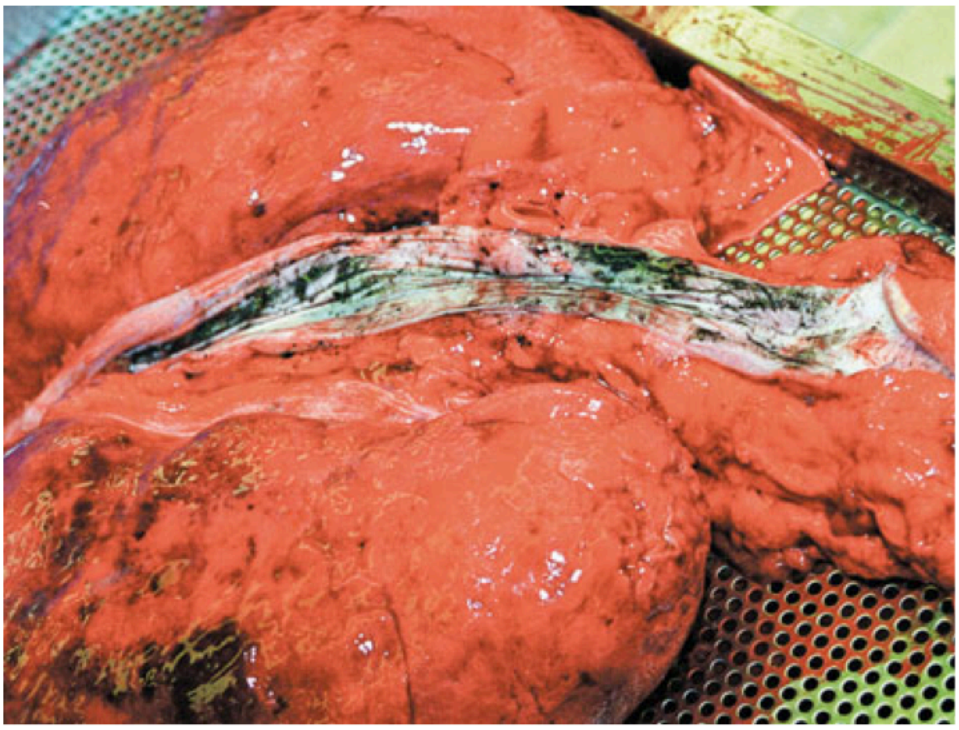

Figure 17.10 Soot staining can be seen in the oesophagus in this body recovered from a house fire. Such staining indicates that the deceased was alive – and able to swallow – at the time of the fire.

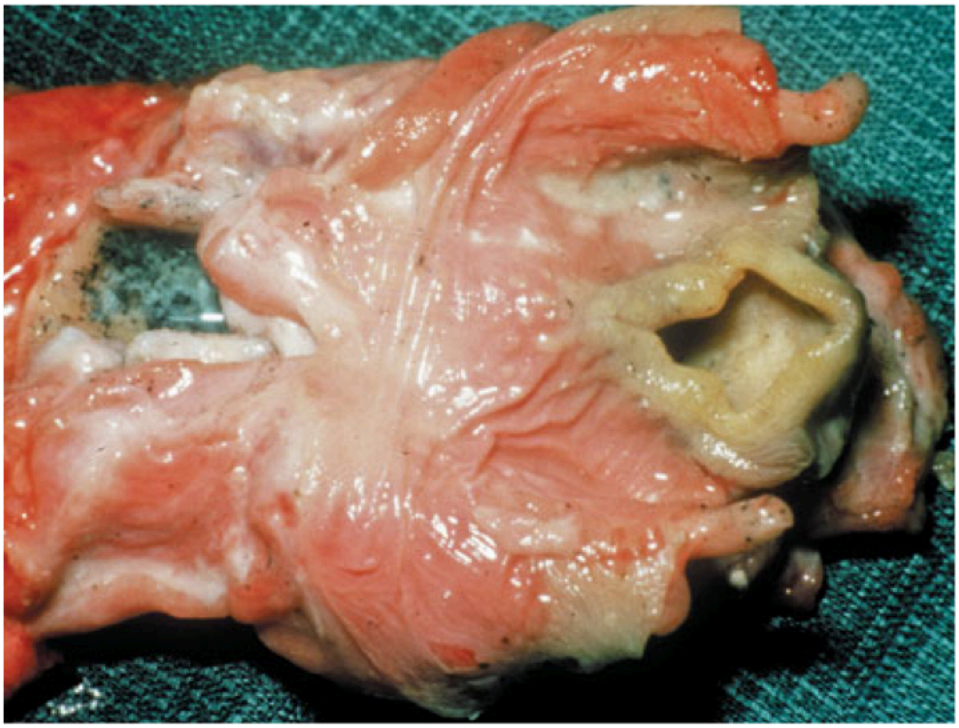

Figure 17.11 Thermal injury to the back of the throat provides evidence of the inhalation of hot gases during a fire, and provides a useful sign of vitality at the time of a fire.

Figure 17.13 Post-mortem artefactual skin splitting in charred skin. No haemorrhage can be seen in the depths of the splits and they should not be confused with ante-mortem injuries.

Figure 17.12 Appearance of 'pugilistic attitude' as a respose to heat effect more on flexor than extensor muscle grasp.

Figure 17.14 Post-mortem fire-related skull fractures in a severely charred body. There is a reddish-brown heat haematoma/extradural haemorrhage on the inner surface of the carbonized cranial vault.

Figure 17.15 Pinkish discoloration over the large joints in fatal hypothermia.

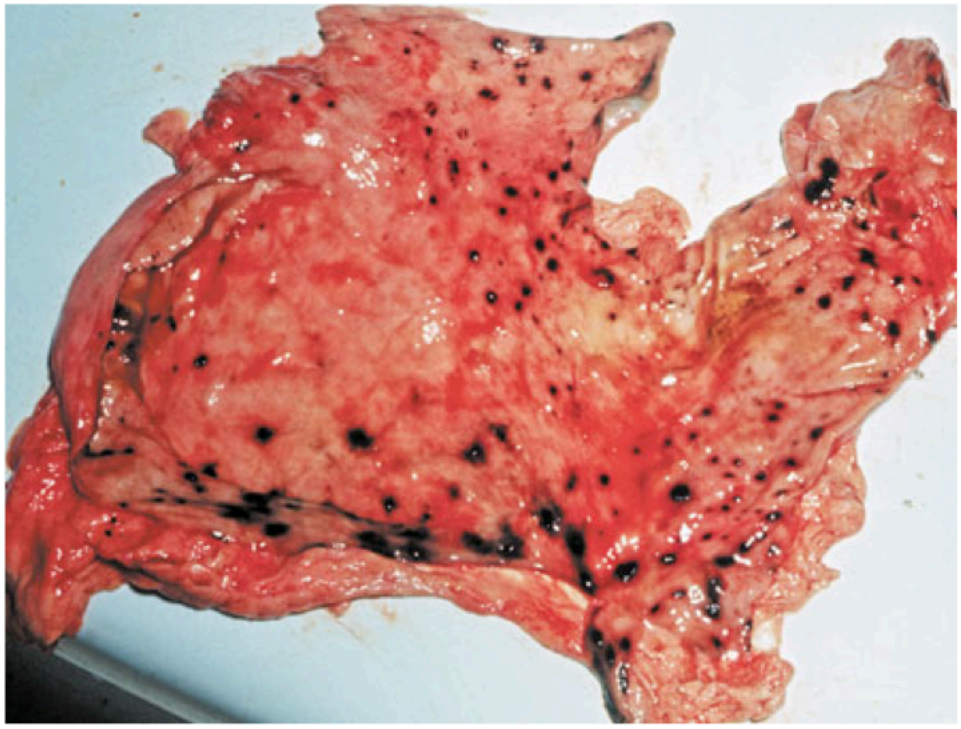

Figure 17.16 Numerous superficial haemorrhagic gastric erosions of the lining of the stomach in hypothermia. These are often called 'Wischnewsky' spots.

Figure 17.17 Frostbite of the knuckles.

Figure 17.19 Multiple electrical marks/burns on the hand, associated with scorching and blistering.

Figure 17.21 The 'Lichtenberg figure' and lightening fatalities. Note the fern-like branching pattern of skin discoloration on the chest.

Figure 17.20 Multiple burns from high-voltage (multi-kilovolt) electrical supply lines. The 'crocodile skin' is caused by arcing of the current over a considerable distance.

Chapter 20: Licit and illicit drugs

Figure 20.1 Multiple drug injection sites.

Figure 20.2 Abscess at site of drug infection.

Figure 20.3 Venous ulcer following deep vein thrombosis secondary to intravenous drug administered into femoral vein.

Figure 20.4 Post-phlebitic limb following repeated injection into femoral vein.

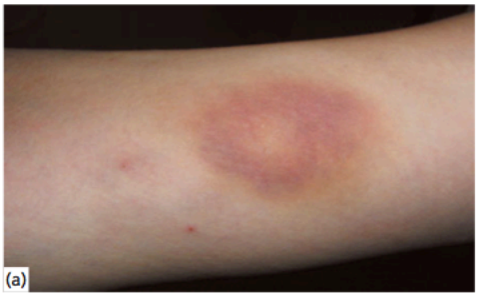

(a)

(b)

(c)

Figure 20.5 Sites of intravenous (IV) injection. **(a)** Forearm; **(b)** foot; **(c)** neck.

Figure 20.6 Cocaine.

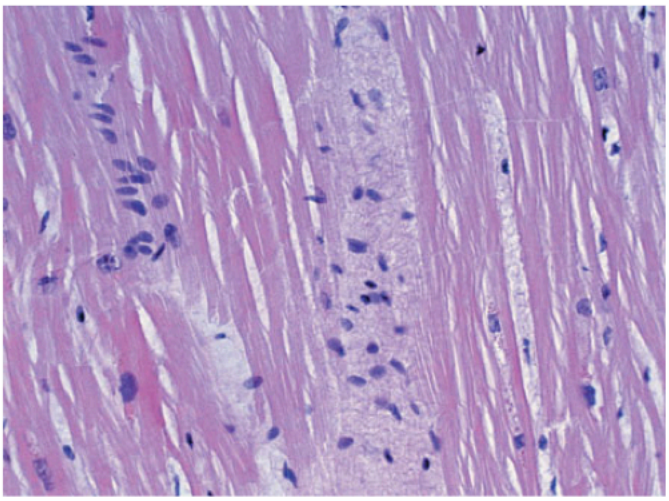

Figure 20.7 Fibrosis of the heart secondary to stimulant abuse.

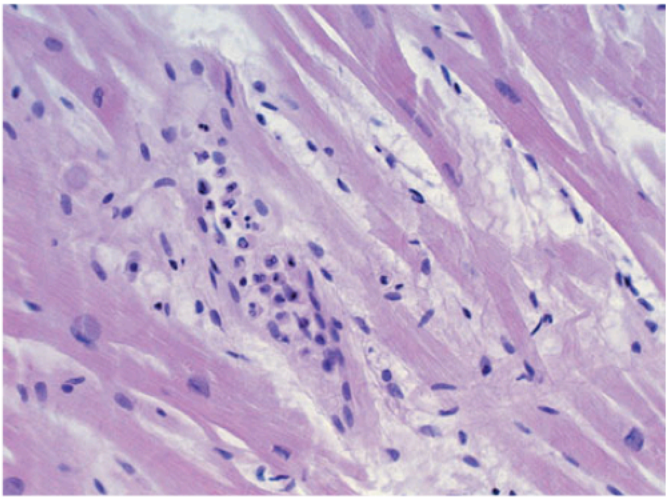

Figure 20.8 Zone of micro-infarction in the heart secondary to stimulant abuse.

Figure 20.9 Khat.

Figure 20.10 Crystal meth.

Figure 20.12 Pinpoint pupils following opiate intake.

Figure 20.13 Track marks from intravenous drug administration.

Chapter 23: Principles of forensic science

Figure 23.2 Sealed and labelled weapon tube containing a bloodstained knife.

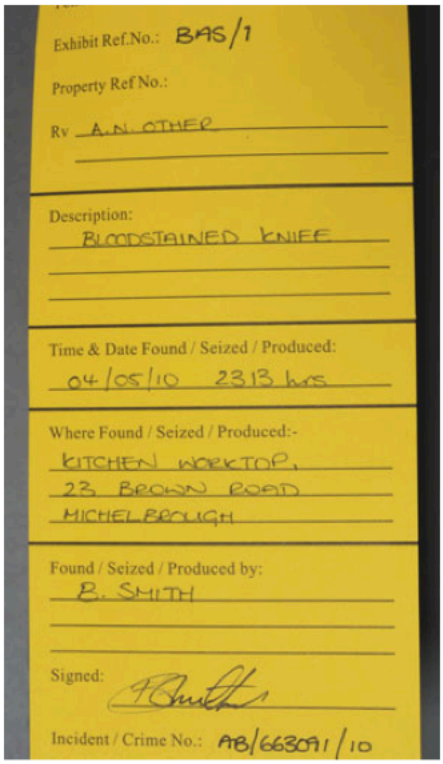

Figure 23.3 A typical exhibit label detailing the unique item number, the item description, the details of where the item was recovered, the time and date on which the item was recovered and the details of the person who recovered the item.

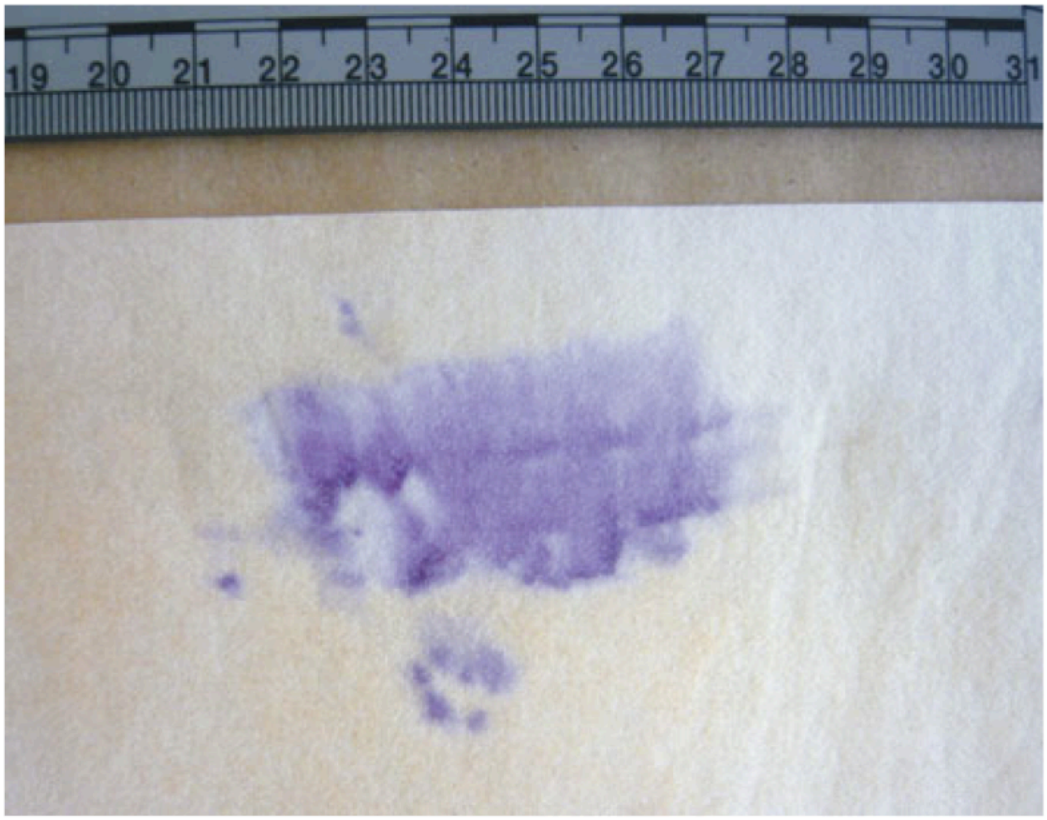

Figure 23.5 A positive reaction result for acid phosphatase (AP), indicating that semen could be present, after application of the AP reagent (photographed at 2 minutes after application).

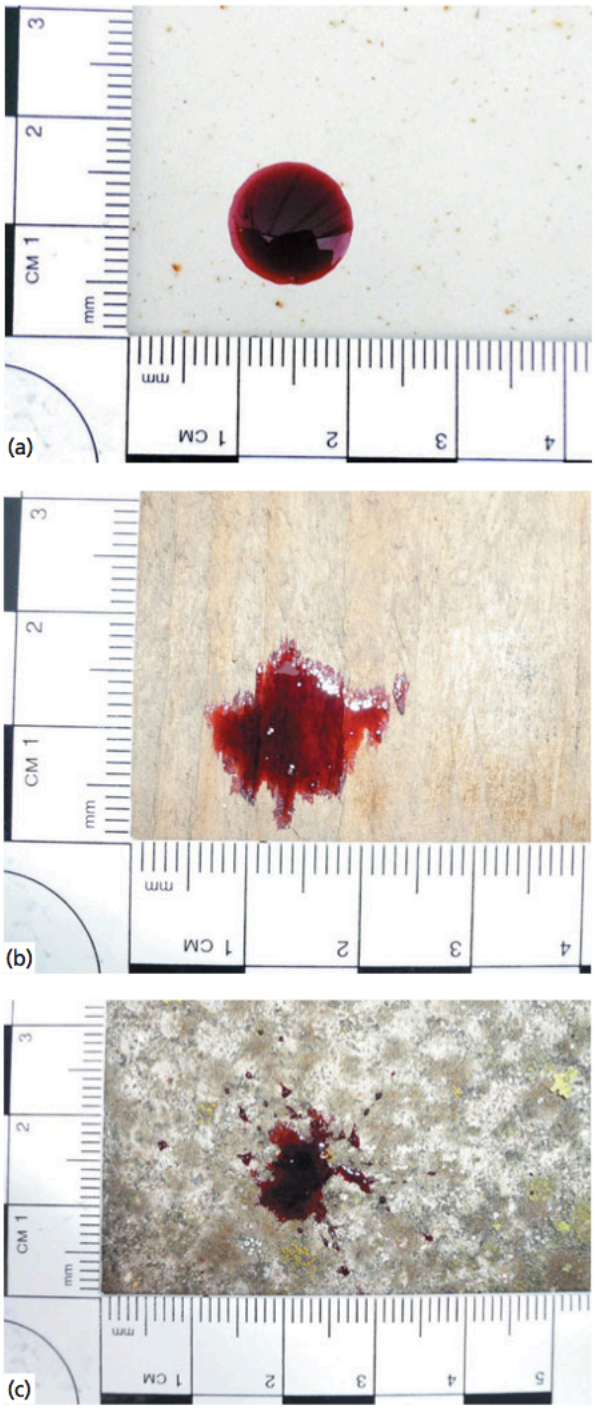

Figure 23.6 Blood dripped onto **(a)** painted metal, **(b)** wood and **(c)** concrete.

Figure 23.7 A contact bloodstain created by a bloodstained hand touching a wall.

Figure 23.8 A typical impact spatter pattern. The source of wet blood was located at the centre of the bottom edge of the picture.

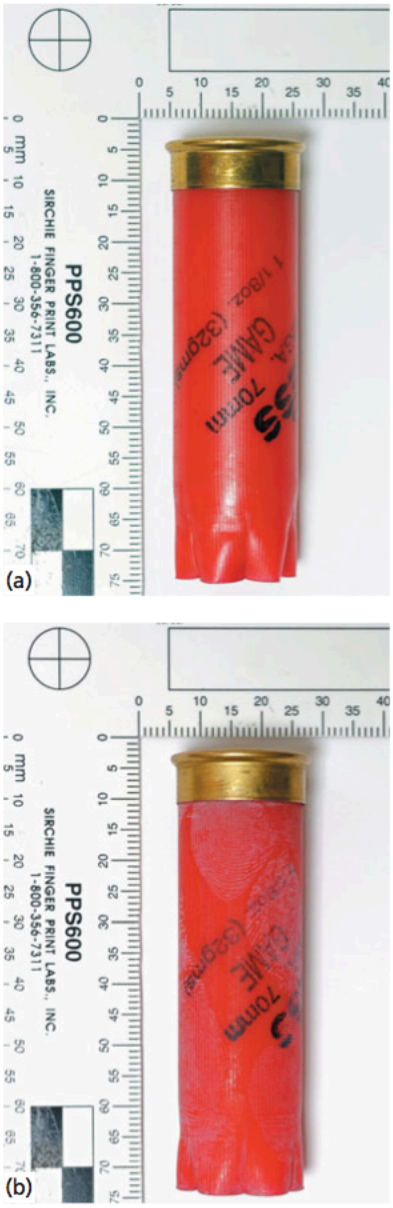

Figure 23.13 A fired shotgun cartridge: **(a)** untreated, and **(b)** treated with cyanoacrylate (superglue) fumes, revealing finger marks.

Figure 23.14 A finger mark in blood left on the blade of a knife. The finger was wet with blood prior to touching the blade.

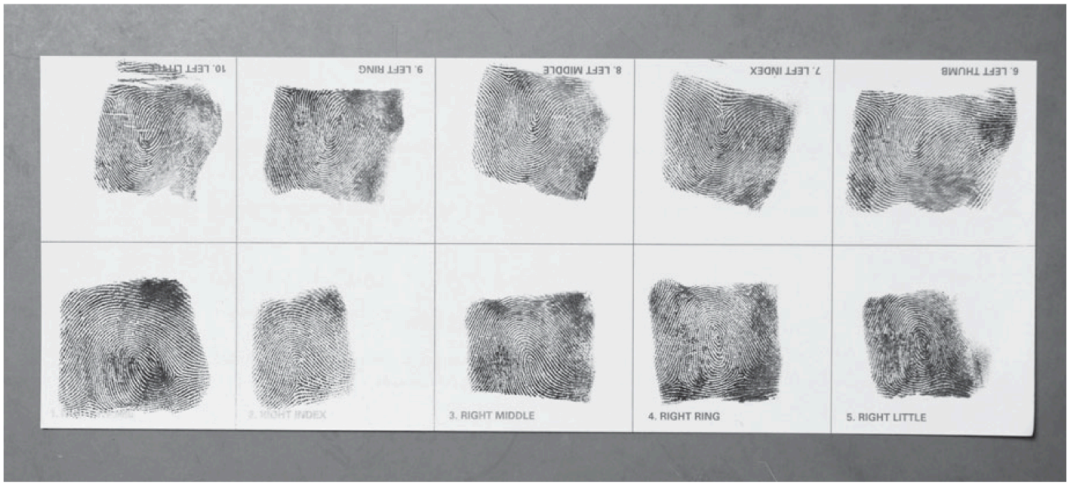

Figure 23.15 Inked fingerprints used as exemplars for comparison.

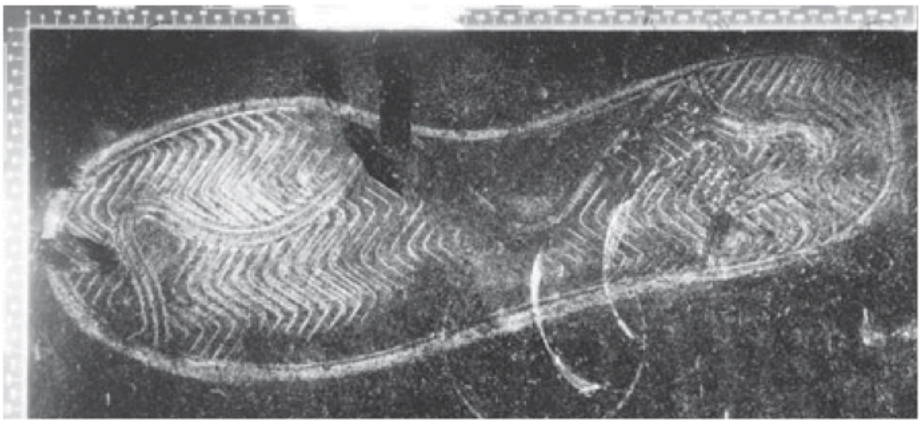

Figure 23.16 Recovered footwear mark showing damage features.

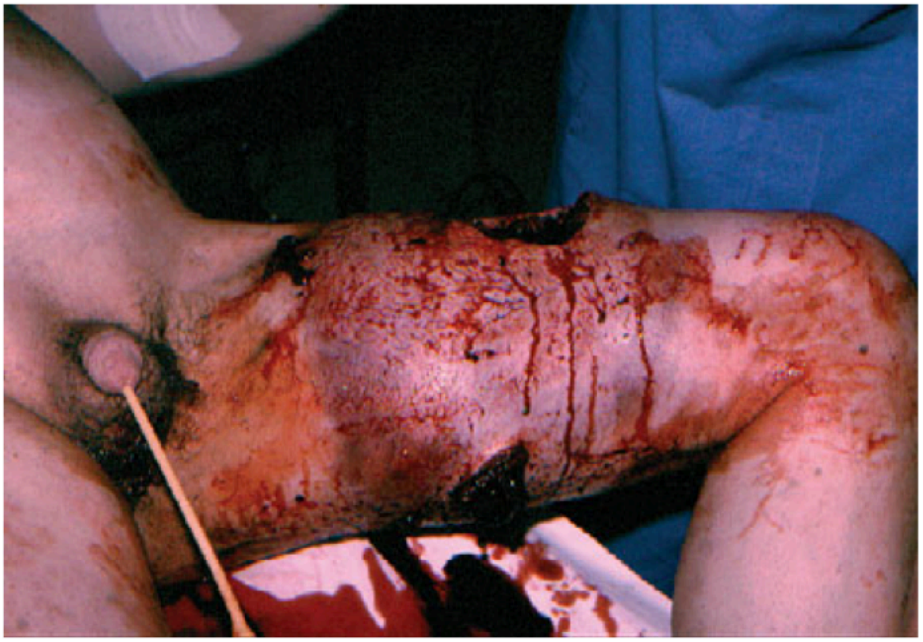

Figure 23.17 Upper thigh injury caused by close range discharge of shotgun to outer leg – bruising, swelling, tissue disruption and lacerations caused by discharge.

Figure 23.18 Revolvers and pistols. **Top:** Heckler & Koch USP (Universal Service Pistol), Germany, 1993. Calibre 9 mm parabellum. **Bottom:** Ruger GP–100, USA, 1987. Calibre .357 Magnum.

Figure 23.19 A 9 × 19 mm Luger semi-automatic pistol cartridge (top), and a NATO 5.56 × 45 mm automatic rifle cartridge (bottom).